J. Fluid Mech. (1979), *vol.* 93, *part* 2, *pp.* 337–377
Printed in Great Britain

Asymptotic properties of Burgers turbulence

By SHIGEO KIDA

Research Institute for Mathematical Sciences, University of Kyoto,
Kyoto 606, Japan

(Received 22 May 1978)

The asymptotic properties of Burgers turbulence at extremely large Reynolds numbers and times are investigated by analysing the exact solution of the Burgers equation, which takes the form of a series of triangular shocks in this situation. The initial probability distribution for the velocity u is assumed to decrease exponentially as $u \to \infty$. The probability distribution functions for the strength and the advance velocity of shocks and the distance between two shocks are obtained and the velocity correlation and the energy spectrum function are derived from these distribution functions. It is proved that the asymptotic properties of turbulence change qualitatively according as the value of the integral scale of the velocity correlation function J, which is invariant in time, is zero, finite or infinite. The turbulent energy per unit length is shown to decay in time t as t^{-1} (with possible logarithmic corrections) or $t^{-\frac{1}{2}}$ according as $J = 0$ or $J \neq 0$.

1. Introduction and summary

It is generally expected that turbulence would have some definite asymptotic properties in the limit of large Reynolds numbers, and to determine such properties is the main objective of the study of turbulence. There are two categories of asymptotic properties. One depends upon the macroscopic structure of the velocity field, which is much influenced by the initial and/or boundary conditions. The other is independent of the details of these conditions. The properties belonging to the former vary from turbulence to turbulence, while those belonging to the latter are universal. Speaking about the three-dimensional Navier–Stokes turbulence, the energy decay law belongs to the former group, whereas the inertial-range spectrum (Kolmogorov 1941, 1962) belongs to the latter.

In the present work we shall deal with Burgers turbulence, intending to work out its asymptotic properties at very large Reynolds numbers. Burgers turbulence has much in common with the Navier–Stokes turbulence, but a definite difference is brought about by the absence of the pressure term in the Burgers equation.

Burgers turbulence has been investigated both analytically and numerically by many authors either as a preliminary approach to turbulence prior to an occurrence of the Navier–Stokes turbulence or for its own sake since the Burgers equation describes the formation and decay of weak shock waves in a compressible fluid (Lighthill 1956; Tatsumi & Tokunaga 1974). As an analytical approach we have a number of theories using different closure assumptions. The cumulant discard hypothesis of Reid (1957) and Kawahara (1968), the Wiener–Hermite expansion of Meecham

0022–1120/79/4213–6930 $02.00

& Siegel (1964), the Lagrangian-history direct-interaction approximation of Kraichnan (1968), the saw-wave expansion of Tatsumi (1969) and Tatsumi & Kida (1972) and the multiple time-scale expansion of Malfliet (1969) and Tatsumi & Mizushima (1979) are only representative examples. The validity of such closure assumptions can be examined by comparing the results due to these assumptions with those due to numerical experiments.

The numerical experiments are made by calculating the solution numerically starting from an arbitrary initial condition. Crow & Canavan (1970) integrated directly the Burgers equation of motion, Jeng *et al.* (1966) calculated the exact form of the solution in terms of the initial data and Hosokawa & Yamamoto (1970) and Yamamoto & Hosokawa (1976) made use of the Monte Carlo quadrature for calculating the exact form. These experiments were made for finite Reynolds numbers and the asymptotic values of various statistical quantities at very large Reynolds numbers were extrapolated.

Looking over all the results of analytical and numerical studies, we find that Burgers turbulence has some definite asymptotic properties at large Reynolds numbers. It seems to have been established at least that the k^{-2} energy spectrum at large wavenumbers is a universal feature of Burgers turbulence and that the energy decay law depends upon macroscopic structure of the velocity field (see Yamamoto & Hosokawa 1976).

Now we would like to analyse Burgers turbulence in an exact manner using no closure assumption and find out its statistical properties at very large Reynolds numbers. Since we are interested in the asymptotic properties in the limit of large Reynolds numbers and times, it is convenient to begin by considering the velocity field in this limit. It is known that the velocity field in this limit is represented by a series of triangular shock waves (Burgers 1950, 1974; Tatsumi & Kida 1972). Each shock has random strength, position and advance velocity. Once their probability distributions are known, all the statistical quantities of the velocity field can be derived from them. For example, the velocity correlation function and the energy spectrum function are derived from the joint probability distribution functions for *two* shocks.

Burgers (1974) tried to calculate these probability distributions by analysing the asymptotic behaviour of the exact form of the solution of the Burgers equation. He dealt with the case in which the integral scale of the velocity correlation function J, defined by (3.6) below, does not vanish. This case will be referred to as case II here. The time-dependence of the characteristic length of the velocity field and the energy decay law were immediately derived by making use of the constancy of J and the dimensional reasoning. The distribution functions for a single shock were obtained in integral form, but they were too complicated to be worked out explicitly. A few lower-order moments of the strength and the advance velocity of a single shock were calculated. By making use of them, the turbulent energy was determined, including a numerical factor. The joint probability distribution functions for two or more shocks were not obtained because of tremendous difficulty in the analysis.

In the present paper we shall mainly deal with the case of vanishing J, which will be referred to as case I here, using a method similar to that of Burgers (1974). It will be shown below that turbulence has qualitatively different properties according as $J \neq 0$ or $J = 0$.

The procedure which is used for obtaining the velocity field in the limit of large Reynolds numbers and times, will be explained briefly in § 2. First, we shall examine the

asymptotic behaviour of the solution of the Burgers equation in this limit, and then give it a geometrical interpretation. The s curve which is an indefinite integral of the initial velocity field and the parabolic arc which includes the time t as a parameter will be introduced. The set of positions of contact points of these two curves determines the velocity field completely. By investigating the probability distribution of this set at every time, we can obtain various statistical quantities which will be discussed in the subsequent sections.

It should be noted that there is no mechanism for producing new randomness in the Burgers equation itself and the randomness can come into the velocity field only through the initial and/or boundary conditions. Since, however, we shall deal with homogeneous turbulence in an infinite domain, only the former condition comes into the problem. The statistical properties of the initial condition will be discussed in § 3. We shall restrict our consideration to the velocity field in which the probability distributions for velocities at two points rapidly become independent as their mutual distance increases so that all moments of the velocity correlation exist. Then the statistical approach becomes different for cases I and II mentioned above. In case II, Burgers expressed the s curve as an Wiener-process along the x axis. In case I, which we are mainly concerned with here, we shall express the s curve as a stationary process.

Statistics of turbulence in case I will be studied in §§ 4–7. We shall deal with the case where the probability density, with which the s curve takes the value y at a point x, decreases exponentially as y goes to infinity [see (4.15)]. The asymptotic properties at large times will be examined and the following results obtained. The approach to the asymptotic state is fastest when $\alpha = 0$ and $\beta = 1$ in (4.15). The number of shocks per unit length of the velocity field decreases as $t^{-\frac{1}{2}}$. Consequently the turbulent energy per unit length decays as t^{-1}. The velocity field assumes a self-preserving structure, that is, all the quantities concerned are invariant in time if they are normalized with reference to the characteristic length and the time. The probability distributions for the strength and the advance velocity of a single shock are mutually independent and they are expressed as (4.38) and (4.39). The joint probability distribution for two adjacent and separated shocks are given by (5.11) and (6.13) respectively. By making use of them we can calculate the probability distributions for the distance between two adjacent and separated shocks as (5.15) and (6.18) respectively and the velocity correlation function as (7.16). This correlation function starts with a positive value at $\tilde{r} = 0$, decreases linearly with $\tilde{r}$ at first, then changes its sign, takes a minimum value and finally approaches zero exponentially. Its Fourier transformation yields the energy spectrum function as (7.24), which is positive definite and changes as $\tilde{k}^2$ and $\tilde{k}^{-2}$ at small and large wavenumbers $\tilde{k}$.

In § 8 we carry out numerical experiments dealing numerically with the velocity field, which is represented by a series of triangular shock waves. For case I, it is shown that experimental results approach the asymptotic state predicted analytically. For case II, we determine numerically the functions which were not obtained explicitly by Burgers (1974), such as the probability distributions for the strength, the advance velocity of a shock and the distance between two shocks, the velocity correlation function and the energy spectrum function. Their curves are depicted in figures 15–19. The standard deviations from these curves are of order of a few per cent on the whole. As for the quantities which have already been obtained by Burgers, they are compared with numerical results. These are the time-dependence of the characteristic length

(figure 12), the energy decay law (figure 13) and a few lower-order moments of the strength and the advance velocity of a shock (tables 2 and 3). It is observed that the agreement is good.

Another consideration about the relation between the time-dependence of the characteristic length and the energy decay law with the initial condition is made in § 9. Lastly the behaviour of the energy spectrum function at small wavenumbers is discussed in connexion with that of the velocity correlation function at large distance.

2. Solution of the Burgers equation

The Burgers equation of motion is written in non-dimensional form as

$$\frac{\partial u}{\partial t}+u\frac{\partial u}{\partial x}=\frac{1}{R}\frac{\partial^2 u}{\partial x^2}, \tag{2.1}$$

where $u(x,t)$ denotes the velocity, x the space co-ordinate, t the time and $R=u_0 l_0/\nu$ the Reynolds number referred to the characteristic velocity u_0 and length l_0 of the initial velocity field and the kinematic viscosity ν.

We shall consider an ensemble of solutions $u(x,t)$ of (2.1) under arbitrary continuous initial conditions $u(x,0)$ specified in an infinite domain $-\infty < x < \infty$. In particular, we are interested in the statistical behaviour of the ensemble of the velocity field $u(x,t)$ for $R \gg 1$ and $t \gg 1$. The behaviours of the solution of (2.1) for very large R and t have already been investigated in detail by Tatsumi & Kida (1972) and Burgers (1974), and we recapitulate them here for later convenience.

The solution under an arbitrary initial condition $u(x,0)$ is expressed in the following integral form (Hopf 1950; Cole 1951):

$$u(x,t)=\frac{\displaystyle\int_{-\infty}^{\infty}\frac{x-x'}{t}\exp\left[-\frac{R}{2}\left\{\frac{(x-x')^2}{2t}+\int_{x_0}^{x'}u(x'',0)\,dx''\right\}\right]dx'}{\displaystyle\int_{-\infty}^{\infty}\exp\left[-\frac{R}{2}\left\{\frac{(x-x')^2}{2t}+\int_{x_0}^{x'}u(x'',0)\,dx''\right\}\right]dx'}, \tag{2.2}$$

where x_0 is an arbitrary constant. When $R \gg 1$, the contribution to the integral essentially comes from the immediate neighbourhood of the point, say X, at which the exponent

$$-\frac{R}{2}\left\{\frac{(x-x')^2}{2t}+\int_{x_0}^{x'}u(x'',0)\,dx''\right\} \tag{2.3}$$

takes an absolute maximum value for fixed x and t. Then we have

$$u(x,t)\approx(x-X)/t. \tag{2.4}$$

It should be noted that (2.4) does not generally represent a straight line since X is a function of x and t. In order to examine the dependence of X on x and t, we introduce the following two curves (figure 1):

$$y=s(x')=-\int_{x_0}^{x'}u(x'',0)\,dx''+s(x_0) \tag{2.5}$$

and

$$y=\frac{(x'-x)^2}{2t}+C. \tag{2.6}$$

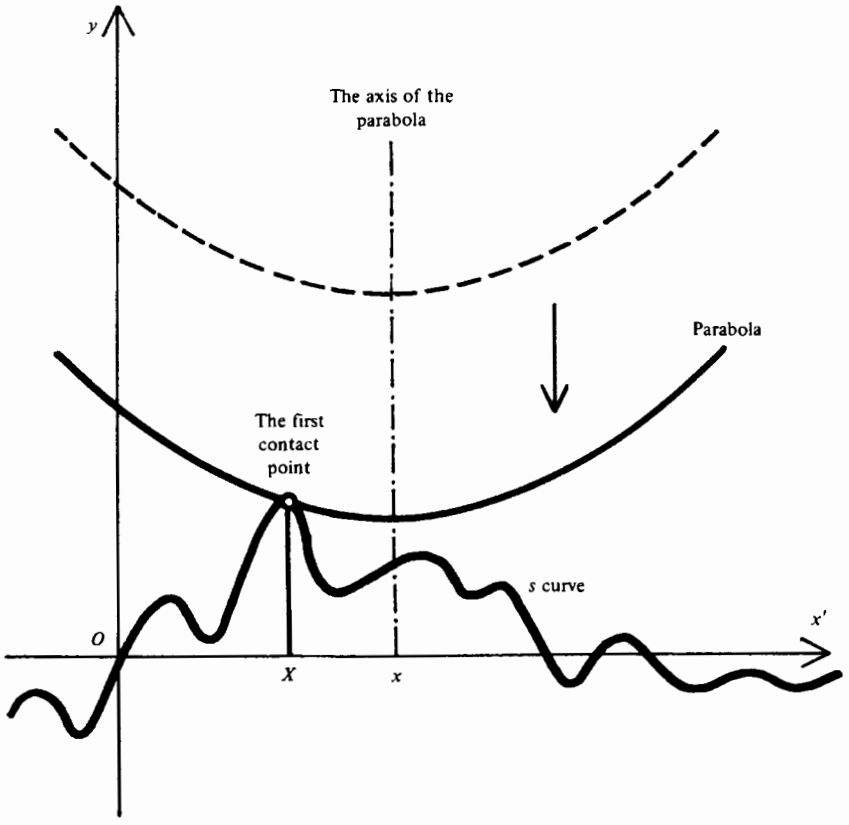

FIGURE 1. The s curve and a contacting parabola.

The form of the s curve (2.5) is completely determined by the initial condition, whereas the parabola given by (2.6), whose axis is the line $x' = x$ and whose vertex becomes flatter with increasing t, is different for different points x and times t. Let us take first the value of C so large that the parabola is well above the s curve, then decrease C until the two curves touch each other for the first time. Then it may easily be seen that the abscissa of the contact point X gives the absolute maximum of (2.3). Making the parabola glide on the s curve, we get the value of X corresponding to each x and thus obtain the velocity $u(x, t)$ as a function of x through (2.4).

Sometimes it happens that the two curves touch simultaneously at two or more points. Since the probability of simultaneous contact at more than two points is negligibly small, we may safely restrict ourselves to the case of double contact. When $t \gg 1$, all contact points come close to the tops of the s curve because then the parabola is much flatter than the s curve (figure 2). Let us denote the abscissa of the ith top of such kind by η_i, where $i = 0, \pm 1, \pm 2, \ldots$ and η_0 is the one closest to the origin. If, for a chosen x, we denote the abscissae of two contact points by X_i and X_{i+1}, the integrals in (2.2) are evaluated as the sum of contributions from the immediate neighbourhoods of X_i and X_{i+1}. Noting that $X_i \approx \eta_i$ and $X_{i+1} \approx \eta_{i+1}$, expanding the function $s(x')$ around η_i and η_{i+1} and evaluating the contributions from the two parts, we obtain

$$u(x,t) = \frac{1}{t}\left(x - \frac{\eta_i + \eta_{i+1}}{2}\right) - \frac{1}{2t}(\eta_{i+1} - \eta_i)\tanh\left\{\frac{R}{4t}(\eta_{i+1} - \eta_i)(x - \xi_i)\right\}, \tag{2.7}$$

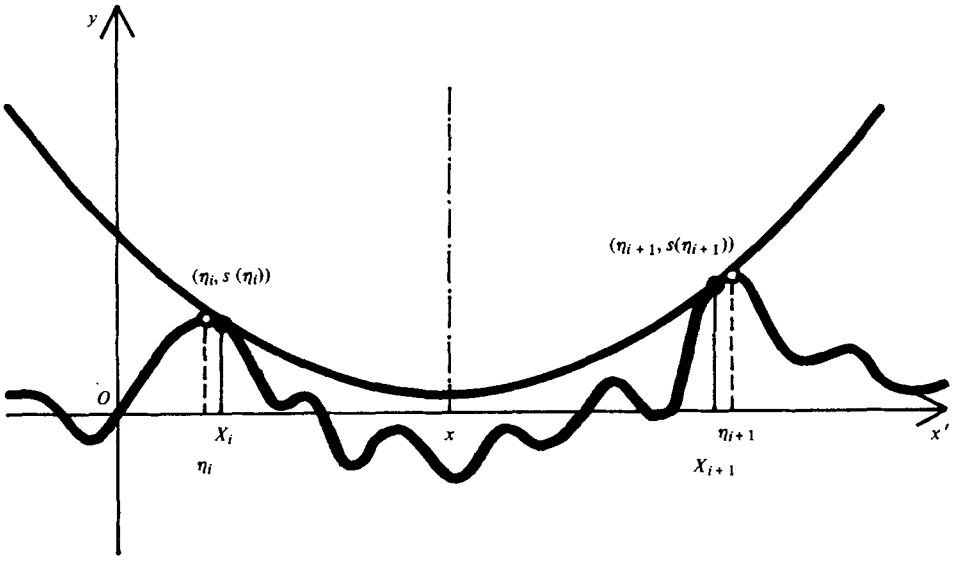

FIGURE 2. A parabola in double contact with the s curve.

where ξ_i is given by

$$\xi_i = \frac{\eta_i+\eta_{i+1}}{2} - \frac{s(\eta_{i+1})-s(\eta_i)}{\eta_{i+1}-\eta_i}t + \frac{t}{R(\eta_{i+1}-\eta_i)}\ln\left(\frac{s''(\eta_{i+1})}{s''(\eta_i)}\right). \tag{2.8}$$

The expression (2.7) is valid in the region $\frac{1}{2}(\xi_{i-1}+\xi_i) < x < \frac{1}{2}(\xi_i+\xi_{i+1})$ and for $R \gg 1$ and $t \gg 1$.

When R is so large that $R \gg t \gg 1$, (2.7) and (2.8) reduce to

$$u(x,t) = \begin{cases} \dfrac{x-\eta_i}{t} & \text{for} \quad \dfrac{\xi_{i-1}+\xi_i}{2} < x < \xi_i, \\ \dfrac{x-\eta_{i+1}}{t} & \text{for} \quad \xi_i < x < \dfrac{\xi_i+\xi_{i+1}}{2} \end{cases} \tag{2.9}$$

and

$$\xi_i = \frac{\eta_{i+1}+\eta_i}{2} - \frac{s(\eta_{i+1})-s(\eta_i)}{\eta_{i+1}-\eta_i}t. \tag{2.10}$$

Equation (2.9) represents a discontinuity or a shock of strength μ_i/t located at ξ_i, where

$$\mu_i = \eta_{i+1}-\eta_i. \tag{2.11}$$

It can easily be shown that the shock moves with the velocity ζ_i/t, where

$$\zeta_i = \xi_i - \frac{\eta_{i+1}+\eta_i}{2}, \tag{2.12}$$

which is equal to the velocity at the centre of the shock. It follows from (2.10) that the co-ordinate ξ_i coincides with the axis of the parabola passing through the two tops $(\eta_i, s(\eta_i))$ and $(\eta_{i+1}, s(\eta_{i+1}))$ of the s curve.

Thus the velocity field in this circumstance is represented by a sequence of vertical lines (shocks) connected by oblique lines of slope $1/t$ (figure 3). The positions of shocks and the intersections of the oblique lines with the x axis are given by $\{\xi_i\}$ and $\{\eta_i\}$ respectively. Each shock moves at a different speed determined by (2.12) and therefore

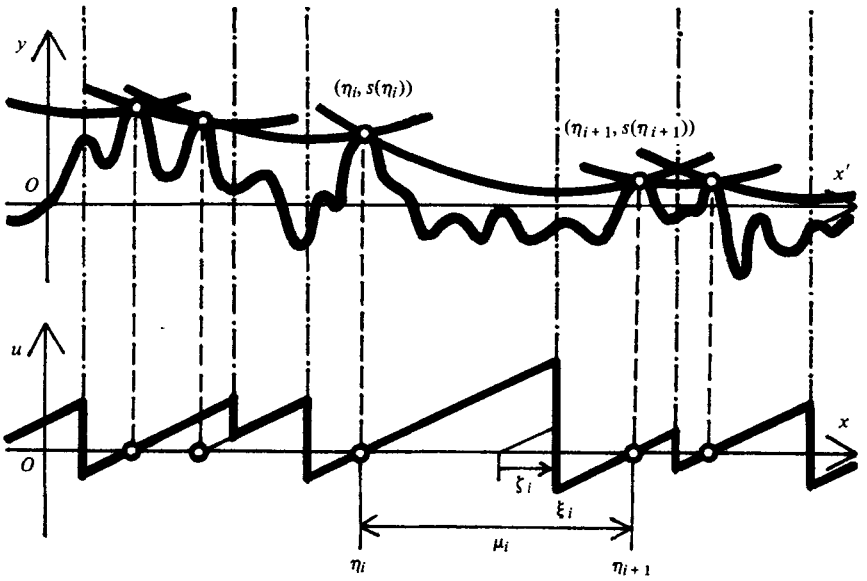

FIGURE 3. A sequence of parabolas in double contact with the s curve and the corresponding velocity field.

they collide with each other from time to time. When two shocks come into collision, they coalesce into one and their strengths are summed. The advance velocity ζ_i/t and the strength of shocks multiplied by t, μ_i are shown to be invariant in time except at the instant of collision, while μ_i and $\mu_i \zeta_i/t$ are conserved at each collision. The above laws of motion enable us to deal with the system of shocks as if it were a collection of cohesive particles, in which each particle is located at ξ_i and has mass μ_i, velocity ζ_i/t and momentum $\mu_i \zeta_i/t$. There is no interaction between particles except at the instants of collisions. All the collisions are perfectly inelastic and the masses and the momentum are conserved at every collision. The only peculiarity of this particle system is that the velocities, the masses and the distance between a pair of adjacent particles are related by (2.12).

Reverting to the picture of the s curve and the parabola, the collision of shocks corresponds to the coalescence of two adjacent parabolic arcs or, in other words, the disappearance of a top of the s curve which used to be in contact with these parabolic arcs. Thus the number of the contact tops of the s curve decreases monotonically in time. Since the system of the tops represents sample points of the arbitrary function $s(x')$, decrease in the number of the tops immediately leads to decrease of arbitrariness of the system. Consequently the randomness of the velocity field can only decrease in time. This property of Burgers turbulence makes an essential contrast to that of the Navier–Stokes turbulence in which the randomness is continuously produced by the nonlinear interaction of vortex filaments and layers. This is the reason why we expect that the statistical properties of Burgers turbulence depend largely upon the initial conditions.

3. Initial condition

Since the velocity field $u(x,t)$ governed by the Burgers equation (2.1) is uniquely determined by the initial field $u(x,0)$, the randomness can come into the field only through the initial condition. We are interested in the statistical behaviour of the turbulent velocity field when an ensemble of initial data $u(x,0)$ or the s curve is given with some prescribed probability distribution. It is assumed that the velocity field is statistically homogeneous and isotropic in space. As a working hypothesis we assume that the initial velocity field has a correlation length χ such that $u(x,0)$ and $u(x',0)$ become independent very rapidly as $|x-x'|$ increases beyond χ. Then, the velocity correlation function

$$B(r,t) = \langle u(x,t)\, u(x+r,t)\rangle \tag{3.1}$$

approaches zero faster than any negative power of r as r goes to infinity at the initial instant. Here $\langle\ \rangle$ represents the average taken over an ensemble of the initial velocity field.

As described in § 2, the velocity field $u(x,t)$ takes the form of a sequence of shocks for $R \gg 1$ and $t \gg 1$. Since the number of shocks decreases through collisions, the characteristic length of the velocity field, which is measured by the mean distance between adjacent shocks, increases monotonically with time. Now that we restrict our attention to the case $t \gg 1$, the length-scale of the parabola, which is measured by the radius of curvature at the vertex, is much longer than that of the s curve. Thus we may take a length-scale which is much longer than that of the s curve but much shorter than that of the parabola.

The mean values of the first and second moments of $s(x)-s(x_0)$ are easily derived from (2.5):

$$\langle s(x)-s(x_0)\rangle = 0 \tag{3.2}$$

and

$$\langle (s(x)-s(x_0))^2\rangle = \int_{x_0}^{x} dx' \int_{x_0}^{x} dx'' \langle u(x',0)\, u(x'',0)\rangle = 2\int_0^{x-x_0} (x-x_0-r)\, B(r,0)\, dr. \tag{3.3}$$

For large values of $|x-x_0|$ ($\gtrsim \chi$), the relation (3.3) is expressed asymptotically as

$$\langle (s(x)-s(x_0))^2\rangle = \begin{cases} -2\int_0^{\infty} rB(r,0)\, dr \sim O(1) & \text{when } J=0 \quad \text{(case I)}, \quad (3.4) \\ 2J|x-x_0| \sim O(|x-x_0|) & \text{when } J \neq 0 \quad \text{(case II)}, \quad (3.5) \end{cases}$$

where

$$J = \int_0^{\infty} B(r,t)\, dr = \int_0^{\infty} B(r,0)\, dr \tag{3.6}$$

is the integral scale of the velocity correlation function. Note that J is invariant in time as easily proved by making use of (2.1) (Burgers 1950). This makes the distinction of the two cases according to the value of J significant for all times.

Case II, $J \neq 0$, was investigated in detail by Burgers (1974). He calculated higher-order moments $\langle (s(x)-s(x_0))^n\rangle$, $n = 3, 4, \ldots$, and found that the s curve is expressed as a Wiener-process along the x axis. By making use of the constancy of J and the dimensional reasoning he obtained the energy decay law. The probability distribution functions for the strength and the advance velocity of shocks were expressed in integral form and a few lower-order moments of them were calculated. However, the complexity of the expression for the probability distribution function prevented him from

working out their forms explicitly. We shall deal with this case in §8.2 and determine these functions numerically as well as other statistical quantities such as the probability distribution functions for the distance between two shocks, the velocity correlation function and the energy spectrum function.

Case I, $J = 0$, will be dealt with in the following sections. We exclude the case where (3.4) vanishes. For, when it does, we have $\langle (s(x)-s(x_0))^2 \rangle = 0$ and $s(x) = s(x_0)$ ($=$ constant) almost everywhere, which corresponds to a trivial velocity field, i.e. $u(x, 0) \equiv 0$. In view of (3.2) and (3.4), it may be a reasonable assumption that the random variable $s(x)-s(x')$ takes values of $O(1)$ whenever $|x-x'| > \chi$. It follows from the definition of $s(x)$ and the independence of the initial velocity field that $s(x)$ and $s(x')$ are independent if $|x-x'| \gg \chi$. So long as the values of $s(x)$ only at points distant from each other by much more than χ are considered, the s curve itself can be regarded as a spatially stationary stochastic process. The corresponding velocity field is essentially equivalent to the one which is expressed by the space derivative of a spatially stationary process (see appendix). The form of the probability distribution function for the s curve is specified as the initial condition.

4. Probability distribution for a single shock

As was mentioned in the preceding section, there exists a length-scale, say Δx, which is much longer than the characteristic length of the s curve which represents the initial velocity field but much shorter than that of the parabolic arcs which is related to the velocity field at the time t. Since the contact points of parabolic arcs on the s curve come close to tops of the s curve for large t, adjacent parabolic arcs are roughly connected at tops of the s curve (see figure 3). We divide the x axis into a number of intervals $I_m = (x_m - \Delta x/2, x_m + \Delta x/2)$, where

$$x_m = m\Delta x, \tag{4.1}$$

m being integers. Denote the ordinate of the highest top of the s curve in the interval I_m by y_m and take (x_m, y_m) as the representative co-ordinate of the contact points in I_m. This approximation may be permissible since the characteristic length of the velocity field under consideration is much longer than Δx. Then the statistical properties of an ensemble of the s curve is described by a set of probability distributions for y_m. Since, on the other hand, Δx is much longer than the characteristic length of the s curve, the probability distribution for y_m in different I_m is supposed to be independent of each other. Thus, we assume that the series of the contact points constitutes a stationary stochastic process along the x-axis, each step of which is *independent*.

Let $P(y)$ be the probability distribution for the ordinates of the highest top of the s curve in each interval normalized as

$$\int_{-\infty}^{\infty} P(y)\,dy = 1. \tag{4.2}$$

Then the number of representative points of the series of contact points within the area $dx\,dy$ around a point (x, y) in the x, y plane is given by

$$\frac{1}{\Delta x} P(y)\,dx\,dy, \tag{4.3}$$

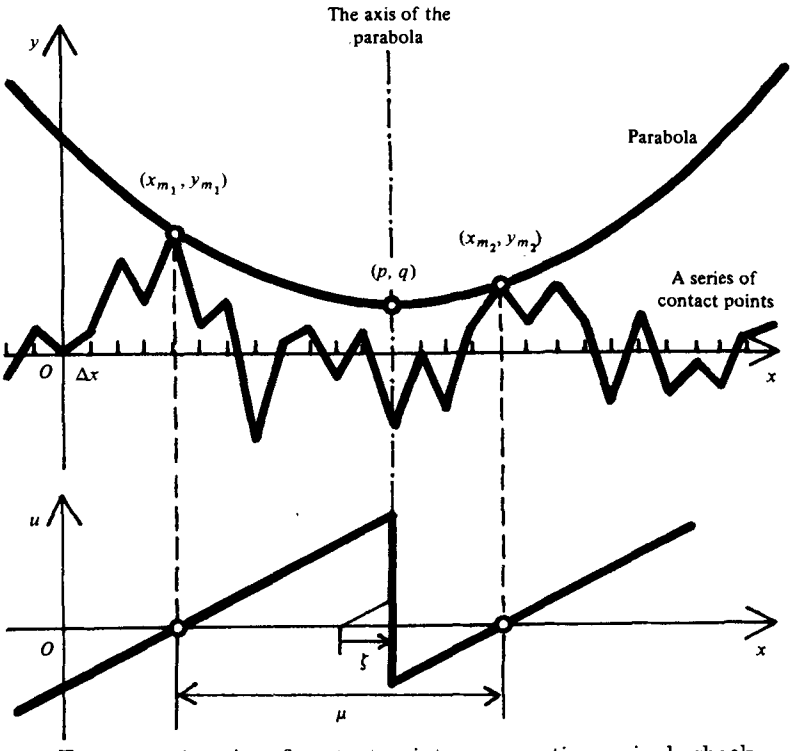

FIGURE 4. A series of contact points representing a single shock.

where $dx, dy \gg \Delta x$ is assumed. If we express the equation of a parabola as

$$y = (x-p)^2/2t + q, \tag{4.4}$$

the number of the series of contact points which pass through two areas $dx_{m_1} dy_{m_1}$ and $dx_{m_2} dy_{m_2}$ respectively around two points (x_{m_1}, y_{m_1}) and (x_{m_2}, y_{m_2}) on the parabola and never go over across it (see figure 4) is given by

$$\frac{1}{(\Delta x)^2} \prod_{j=1}^{2} P(y_{m_j})\, dx_{m_j}\, dy_{m_j} \prod_{i \neq m_1, m_2} \{1 - F(y_i)\}, \tag{4.5}$$

where

$$y_i = \frac{1}{2t}(x_i - p)^2 + q, \quad F(y) = \int_y^\infty P(y')\, dy'. \tag{4.6), (4.7}$$

It should be noted that the polygonal line in figure 4 represents a sequence of contact points, not the s curve itself. The picture of the corresponding shock is shown in the lower part of figure 4. The position of the shock is given by the axis of the parabola. Making reference to (2.10)–(2.12), we find that the strength μ/t and the advance velocity ζ/t of the shock are given by

$$\mu/t = (x_{m_2} - x_{m_1})/t, \tag{4.8}$$

$$\zeta/t = -(y_{m_2} - y_{m_1})/(x_{m_2} - x_{m_1}). \tag{4.9}$$

The vertex (p, q) of the parabola is written as

$$p = x_{m_1} + \zeta + \frac{\mu}{2}, \quad q = y_{m_1} - \frac{1}{2t}\left(\zeta + \frac{\mu}{2}\right)^2, \tag{4.10), (4.11}$$

where use has been made of (4.6), (4.8) and (4.9).

Replacing the independent variables in (4.5) by μ, ζ through (4.8)–(4.11), we obtain the number density of shocks per unit length whose strength lies between μ/t and $(\mu+d\mu)/t$ and advance velocity between ζ/t and $(\zeta+d\zeta)/t$ as follows:

$$n(\mu,\zeta;t)\,d\mu\,d\zeta = \frac{d\mu\,d\zeta}{(\Delta x)^2}\frac{\mu}{t}\int_{-\infty}^{\infty} P(y_{m_1})\,P\left(y_{m_1}-\frac{\mu\zeta}{t}\right)\prod_{i\neq m_1,m_2}\{1-F(y_i)\}\,dy_{m_1}. \quad (4.12)$$

When t is large, the factor

$$\prod_{i\neq m_1,m_2}\{1-F(y_i)\}$$

may be approximated by an integral, and (4.12) is written as

$$n(\mu,\zeta;t) = \frac{1}{(\Delta x)^2}\frac{\mu}{t}\int_{-\infty}^{\infty}\frac{P(y)}{1-F(y)}\,\frac{P(y-\mu\zeta/t)}{1-F(y-\mu\zeta/t)}\exp\left[\frac{\sqrt{(2t)}}{\Delta x}\int_{-\infty}^{\infty}\ln\{1-F(x^2+q)\}\,dx\right]dy, \quad (4.13)$$

where

$$q = y-\frac{1}{2t}\left(\zeta+\frac{\mu}{2}\right)^2. \quad (4.14)$$

The integrand of (4.13) for large t has a peak at some point, say $y=\bar{y}$, which is much larger than $\langle y^2\rangle^{\frac{1}{2}}$, the standard deviation of $P(y)$. This can be proved straightforwardly if $P(y)$ approaches zero exponentially or algebraically as y goes to infinity.

When $P(y)$ has an exponential tail, the peak is localized and the integration can be estimated by making use of the method of steepest descent. In the following we shall consider this case.† Put $P(y)$ as

$$P(y) \approx \Delta x A y^{\alpha}\exp(-By^{\beta}) \quad \text{for} \quad y \gg \langle y^2\rangle^{\frac{1}{2}}, \quad (4.15)‡$$

where A, B, β are positive constants and α is an arbitrary one. As will be shown later, the parameters B and β in the exponent play important roles, whereas A and α do only minor ones. First we assume that the saddle point which gives the peak of the integrand of (4.13) lies in the region $y \gg \langle y^2\rangle^{\frac{1}{2}}$ and $y \gg \mu\zeta/t$, and then show that the results are consistent with this assumption.

Since $F(y) \ll 1$ for $y \gg \langle y^2\rangle^{\frac{1}{2}}$, (4.13) is approximated by

$$n(\mu,\zeta;t) = \frac{1}{(\Delta x)^2}\frac{\mu}{t}\int_{-\infty}^{\infty} P(y)\,P\left(y-\frac{\mu\zeta}{t}\right)\exp\left\{-\frac{\sqrt{(2t)}}{\Delta x}\int_{-\infty}^{\infty}F(x^2+q)\,dx\right\}dy, \quad (4.16)$$

which is rewritten as

$$n(\mu,\zeta;t) = \frac{1}{(\Delta x)^2}\frac{\mu}{t}\int_{-\infty}^{\infty}\exp\{\Phi(y)\}\,dy, \quad (4.17)$$

where

$$\Phi(y) = \ln\left\{P(y)\,P\left(y-\frac{\mu\zeta}{t}\right)\right\}-\frac{\sqrt{(2t)}}{\Delta x}\int_{-\infty}^{\infty}F(x^2+q)\,dx. \quad (4.18)$$

If we denote the saddle point of $\Phi(y)$ by $\bar{y}$, we have

$$\left(\frac{d\Phi}{dy}\right)_{y=\bar{y}} = \frac{P'(\bar{y})}{P(\bar{y})}+\frac{P'(\bar{y}-\mu\zeta/t)}{P(\bar{y}-\mu\zeta/t)}+\frac{\sqrt{(2t)}}{\Delta x}\int_{-\infty}^{\infty}P(x^2+\bar{q})\,dx = 0, \quad (4.19)$$

† When $P(y)$ vanishes algebraically, the peak is not localized and the above method is unavailable. Instead, direct integration can be performed in terms of only the asymptotic form of $P(y)$ (see appendix).

‡ It is obvious from the definition that the distribution functions $P(y)$ for different widths Δx are connected by the relation $P_{n\Delta x}(y) = nP_{\Delta x}(y)\{1-F_{\Delta x}(y)\}^{n-1}$, where subscripts denote the width. For large y, this becomes $P_{n\Delta x}(y) = nP_{\Delta x}(y)$, i.e. $P_{\Delta x}(y)$ is proportional to Δx.

where
$$\bar{q} = \bar{y} - \frac{1}{2t}\left(\zeta + \frac{\mu}{2}\right)^2. \tag{4.20}$$

It follows from (4.15) that, when $y \gg \langle y^2\rangle^{\frac{1}{2}}$ and $y \gg \mu\zeta/t$,

$$\frac{P'(y)}{P(y)} \approx \frac{P'(y-\mu\zeta/t)}{P(y-\mu\zeta/t)} \approx -B\beta y^{\beta-1} \approx -B\beta q^{\beta-1}, \tag{4.21}$$

$$\int_{-\infty}^{\infty} P(x^2+q)\,dx \approx \Delta x A \left(\frac{\pi}{B\beta}\right)^{\frac{1}{2}} q^{\alpha-\frac{1}{2}(\beta-1)} \exp\left(-Bq^{\beta}\right), \tag{4.22}$$

$$\int_{-\infty}^{\infty} F(x^2+q)\,dx \approx \frac{\Delta x A \pi^{\frac{1}{2}}}{(B\beta)^{\frac{3}{2}}} q^{\alpha-\frac{3}{2}(\beta-1)} \exp\left(-Bq^{\beta}\right). \tag{4.23}$$

When $\alpha = 0$ and $\beta = 1$, these relations are exact, otherwise the errors are $O(y^{-\beta}, y^{-1})$. Substitution from (4.21) and (4.22) into (4.19) yields

$$\left(\frac{d\Phi}{dy}\right)_{y=\bar{y}} = -2B\beta\bar{q}^{\beta-1} + A\left(\frac{2\pi t}{B\beta}\right)^{\frac{1}{2}} \bar{q}^{\alpha-\frac{1}{2}(\beta-1)} \exp\left(-B\bar{q}^{\beta}\right) = 0, \tag{4.24}$$

which has the asymptotic solution

$$B\bar{q}^{\beta} \approx \ln\left\{A\left(\frac{\pi t}{2}\right)^{\frac{1}{2}} \beta^{-\frac{1}{2}} B^{-(2\alpha+3)/2\beta}\right\} \quad \text{for large } t. \tag{4.25}$$

This tells us that $\bar{q}$ and therefore $\bar{y}$ increase with t, which is consistent with the *a priori* assumption $\bar{y} \gg \langle y^2\rangle^{\frac{1}{2}}$.

We transform the integration variable as

$$y = \bar{y} + Cy', \tag{4.26}$$

where C is a constant. Approximating (4.15) and (4.23) to the lowest order of y' and substituting them into (4.17) and (4.18), we obtain

$$n(\mu,\zeta;t) = CA^2\frac{\mu}{t}\bar{q}^{2\alpha}\exp\left(-2B\bar{q}^{\beta}\right) \times \int_{-\infty}^{\infty} \exp\left\{-B\beta\bar{q}^{\beta-1}\left(\frac{\mu^2}{4t} + \frac{\zeta^2}{t} + 2Cy'\right) - 2\exp\left(-B\beta\bar{q}^{\beta-1}Cy'\right)\right\} dy', \tag{4.27}$$

where (4.20) and (4.24) are used. Here we introduce new variables

$$l(t) = \left(\frac{\pi t}{B\beta}\right)^{\frac{1}{2}} \bar{q}^{\frac{1}{2}(1-\beta)}, \tag{4.28}$$

$$\tilde{\mu} = \frac{\mu}{l(t)}, \tag{4.29}\dagger$$

$$\tilde{\zeta} = \frac{\zeta}{l(t)} \tag{4.30}$$

and put
$$C = \frac{l(t)^2}{\pi t}. \tag{4.31}$$

† Except for in §8.2 the variables $\tilde{\mu}$, $\tilde{\zeta}$, $\tilde{\lambda}$, $\tilde{r}$ defined here and later stand for the corresponding ones measured by $l(t)$ and $\tilde{n}, \tilde{f}, \tilde{g}_a, \tilde{g}_s, \tilde{g}, \tilde{h}$ the functions of these variables.

Then (4.24) becomes

$$A^2\bar{q}^{2\alpha}\exp(-2B\bar{q}^{\beta}) = \frac{2(B\beta)^3}{\pi t}\bar{q}^{3(\beta-1)} = \frac{2\pi^2 t^2}{l(t)^6}. \tag{4.32}$$

By making use of (4.29)–(4.32), we can calculate (4.27) to be

$$\tilde{n}(\tilde{\mu},\tilde{\zeta};t) = l(t)^2 n(\mu,\zeta;t) = \frac{\pi}{2l(t)}\tilde{\mu}\exp\left\{-\pi\left(\frac{\tilde{\mu}^2}{4}+\tilde{\zeta}^2\right)\right\}, \tag{4.33}$$

which is the number density of a single shock of $(\tilde{\mu},\tilde{\zeta})$.† This is exact again when $\alpha = 0$ and $\beta = 1$. It follows from (4.20), (4.25), (4.28) and (4.31) that $C/\bar{y} \approx 1/\ln t \ll 1$ for large t, which implies that the peak of the integrand of (4.13) is actually localized. Equation (4.33) shows that the probability distributions for $\tilde{\mu}$ and $\tilde{\zeta}$ of a single shock are independent of each other and that the time enters only through $l(t)$, i.e. it is similar with respect to time.

Integration of (4.33) with respect to $\tilde{\mu}$ and $\tilde{\zeta}$ yields the number of shocks per unit length:

$$N(t) = \int_0^\infty d\tilde{\mu}\int_{-\infty}^{\infty} d\tilde{\zeta}\,\tilde{n}(\tilde{\mu},\tilde{\zeta}) = \frac{1}{l(t)}, \tag{4.34}$$

which shows that $l(t)$ is the mean distance between adjacent shocks. The mean distance $l(t)$ is calculated by substituting $\bar{q}$ determined by (4.24) into (4.28). Its leading term is written as

$$l(t) \approx \left(\frac{\pi t}{B^{1/\beta}\beta}\right)^{\frac{1}{2}}\left[\ln\left\{A\left(\frac{\pi t}{2}\right)^{\frac{1}{2}}\beta^{-\frac{1}{2}}B^{-(2\alpha+3)/2\beta}\right\}\right]^{(1-\beta)/2\beta}, \tag{4.35}$$

where use has been made of (4.25). It can be seen that (4.35) becomes

$$l(t) \propto t^{\frac{1}{2}} \tag{4.36}$$

for large values of t, which is exact when $\beta = 1$ and asymptotically valid when $\beta \neq 1$. This time-dependence of $l(t)$ is characteristic of Burgers turbulence for $J = 0$. The energy decay law is immediately derived from it [see (7.12)]. Incidentally it is known that the mean distance changes in a quite different way in the case $J \neq 0$ [see (8.3)].

Dividing (4.33) by $N(t)$, we obtain the probability distribution density $\tilde{f}(\tilde{\mu},\tilde{\zeta})$ of finding a shock of $(\tilde{\mu},\tilde{\zeta})$:

$$\tilde{f}(\tilde{\mu},\tilde{\zeta}) = \tfrac{1}{2}\pi\tilde{\mu}\exp\{-\pi(\tfrac{1}{4}\tilde{\mu}^2+\tilde{\zeta}^2)\} = \tilde{f}(\tilde{\mu})\,\tilde{h}(\tilde{\zeta}), \tag{4.37}$$

where

$$\tilde{f}(\tilde{\mu}) = \tfrac{1}{2}\pi\tilde{\mu}\exp(-\tfrac{1}{4}\pi\tilde{\mu}^2) \tag{4.38}$$

and

$$\tilde{h}(\tilde{\zeta}) = \exp(-\pi\tilde{\zeta}^2) \tag{4.39}$$

are the probability distribution densities for the strength and the advance velocity of shocks. They are shown graphically in figures 5 and 6, respectively. Note that these functions do not depend upon the time explicitly.

The moments of $\tilde{\mu}$ and $\tilde{\zeta}$ for (4.37) are easily calculated as

$$\langle\tilde{\mu}^m\tilde{\zeta}^n\rangle = \langle\tilde{\mu}^m\rangle\langle\tilde{\zeta}^n\rangle = \begin{cases} \dfrac{2^m}{\pi^{\frac{1}{2}(m+n+1)}}\Gamma(\tfrac{1}{2}m+1)\,\Gamma(\tfrac{1}{2}(n+1)) & \text{when } n \text{ is even,} \\ 0 & \text{when } n \text{ is odd,} \end{cases} \tag{4.40}$$

† The notation $(\tilde{\mu},\tilde{\zeta})$ denotes a shock having the strength $l(t)\,\tilde{\mu}/t$ and the advance velocity $l(t)\,\tilde{\zeta}/t$.

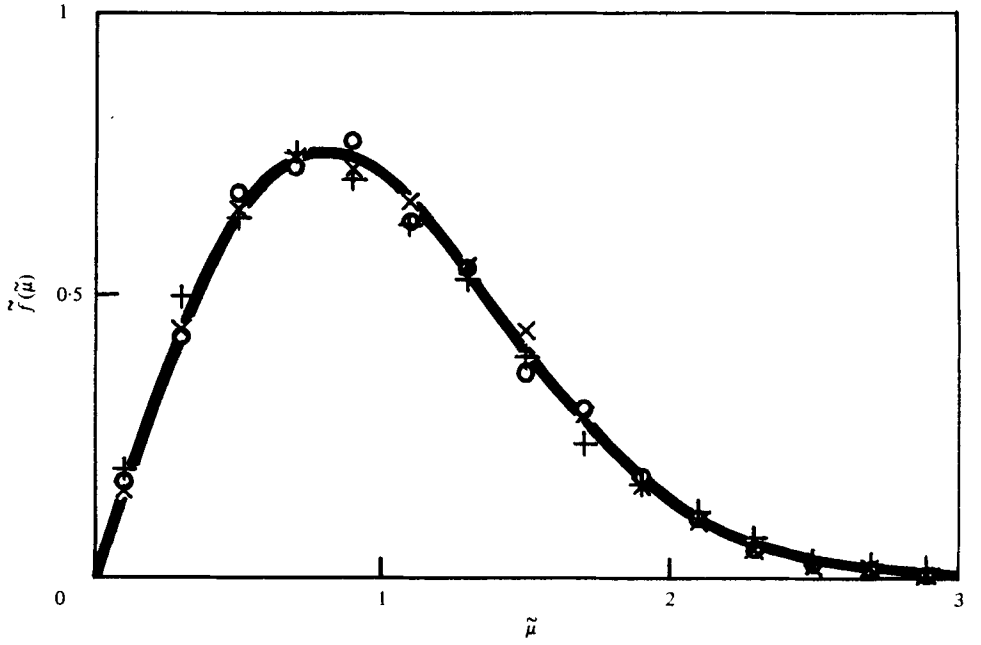

FIGURE 5. The probability distribution for the strength of shocks in case I. The marks +, ○, indicate respectively the numerical results in experiments (i), (ii) and (iii) made in §8.1.

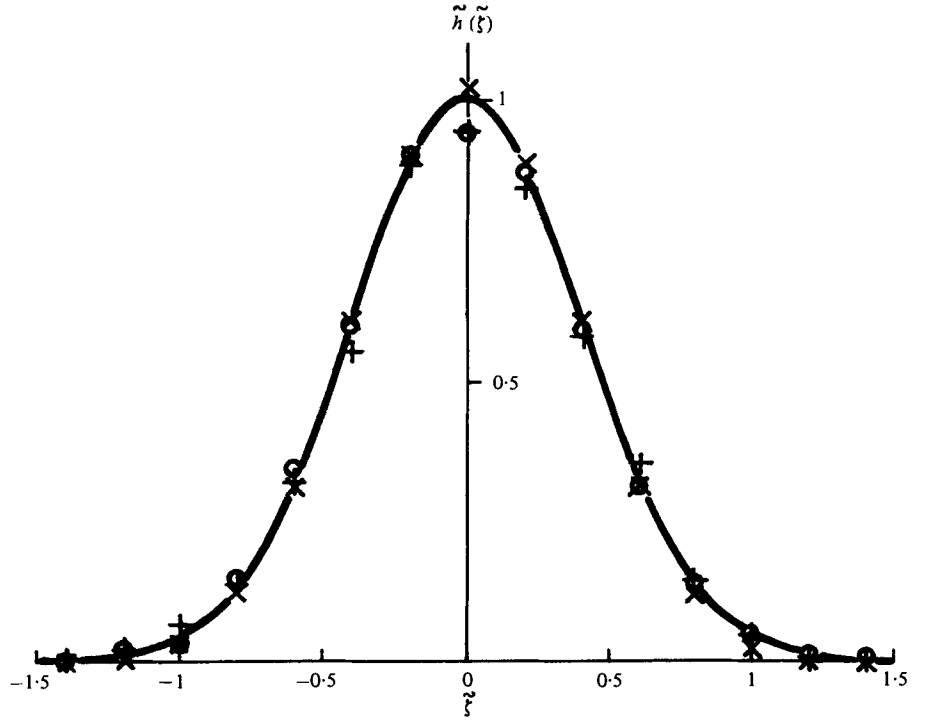

FIGURE 6. The probability distribution for the advance velocity of shocks in case I.

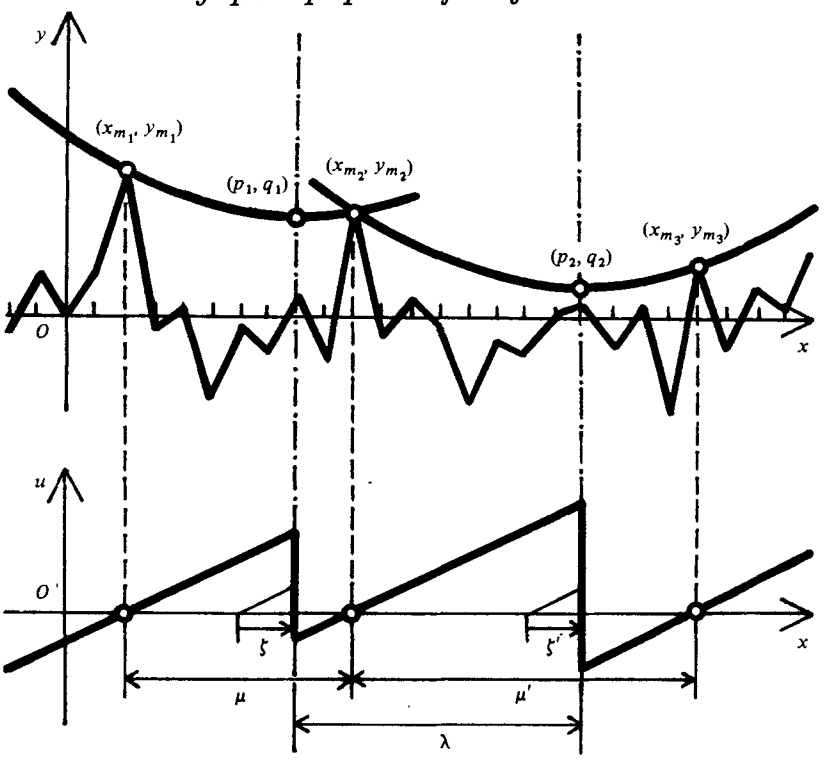

FIGURE 7. A series of contact points representing two adjacent shocks.

where Γ is the gamma function. The first few of them are

$$\left.\begin{aligned} &\langle\tilde{\mu}\rangle = 1, \quad \langle\tilde{\mu}^2\rangle = \frac{4}{\pi}, \quad \langle\tilde{\mu}^3\rangle = \frac{6}{\pi}, \quad \langle\tilde{\mu}^4\rangle = \frac{32}{\pi^2}, \quad \langle\tilde{\mu}^5\rangle = \frac{60}{\pi^2}, \\ &\langle\tilde{\zeta}\rangle = 0, \quad \langle\tilde{\zeta}^2\rangle = \frac{1}{2\pi}, \quad \langle\tilde{\zeta}^3\rangle = 0, \quad \langle\tilde{\zeta}^4\rangle = \frac{3}{4\pi^2}, \quad \langle\tilde{\zeta}^5\rangle = 0. \end{aligned}\right\} \tag{4.41}$$

The first of (4.41) reflects the fact that the mean distance between adjacent shocks is chosen as a unit of length.

5. Joint probability distribution for two adjacent shocks

In order to calculate the velocity correlation function and the energy spectrum function it is necessary to know the joint probability distributions for a pair of shocks. A pair of shocks are classified into two groups according as they adjoin each other or contain other shocks between them. We shall refer to the former pair as 'two adjacent shocks' and to the latter as 'two separated shocks' and deal with them in this section and in the next section respectively.

Two adjacent shocks are represented by a series of contact points which passes through the intersection of two adjacent parabolas and contacts again with each parabola at other points and runs below both parabolas at all the other points as illustrated in figure 7.

Let us express the equation of the two parabolas by

$$y = \frac{(x-p_1)^2}{2t} + q_1, \tag{5.1}$$

$$y = \frac{(x-p_2)^2}{2t} + q_2, \tag{5.2}$$

where $p_1 < p_2$, and denote the co-ordinate of their intersection by (x_{m_2}, y_{m_2}). The axes of these parabolas p_1 and p_2 indicate the positions of the two shocks. The number of the series of contact points which pass through the area $dx_{m_1}\,dy_{m_1}$ around a point (x_{m_1}, y_{m_1}) on the left parabola, $dx_{m_2}\,dy_{m_2}$ around the intersection (x_{m_2}, y_{m_2}) and $dx_{m_3}\,dy_{m_3}$ around a point (x_{m_3}, y_{m_3}) on the right parabola and below both parabolas at all the other points is given by

$$\frac{1}{(\Delta x)^3} \prod_{j=1}^{3} P(y_{mj})\,dx_{m_j}\,dy_{m_j} \prod_{i \neq m_1, m_2, m_3} \{1-F(y_i)\}, \tag{5.3}$$

where

$$y_i = \begin{cases} \dfrac{1}{2t}(x_i-p_1)^2 + q_1 & \text{for} \quad x_i \leqslant x_{m_2}, \\ \dfrac{1}{2t}(x_i-p_2)^2 + q_2 & \text{for} \quad x_i > x_{m_2}. \end{cases} \tag{5.4}$$

When there are two shocks (μ, ζ)† and (μ', ζ') at p_1 and p_2 respectively, by making reference to (4.8)–(4.11), we find the following relations:

$$\mu = x_{m_2} - x_{m_1}, \quad \mu' = x_{m_3} - x_{m_2}, \tag{5.5}$$

$$\frac{\mu\zeta}{t} = y_{m_1} - y_{m_2}, \quad \frac{\mu'\zeta'}{t} = y_{m_2} - y_{m_3}, \tag{5.6}$$

$$p_1 = x_{m_2} + \zeta - \frac{\mu}{2}, \quad p_2 = x_{m_2} + \zeta' + \frac{\mu'}{2}, \tag{5.7}$$

$$q_1 = y_{m_2} - \frac{1}{2t}\left(\zeta - \frac{\mu}{2}\right)^2, \quad q_2 = y_{m_2} - \frac{1}{2t}\left(\zeta' + \frac{\mu'}{2}\right)^2. \tag{5.8}$$

The distance λ between the two shocks is given by

$$\lambda = p_2 - p_1 = \zeta' - \zeta + \tfrac{1}{2}(\mu+\mu')\,(> 0), \tag{5.9}$$

where (5.7) has been used.

Rewriting (5.3) in terms of μ, μ', ζ, ζ' through (5.5)–(5.8), we get the number density of two adjacent shocks (μ, ζ) and (μ', ζ'):

$$n_a(\mu, \zeta; \mu', \zeta'; t) = \begin{cases} \dfrac{1}{(\Delta x)^3}\dfrac{\mu\mu'}{t^2} \displaystyle\int_{-\infty}^{\infty} \frac{P(y+(\mu\zeta/t))}{1-F(y+(\mu\zeta/t))} \frac{P(y)}{1-F(y)} \frac{P(y-(\mu'\zeta'/t))}{1-F(y-(\mu'\zeta'/t))} \\ \quad \times \exp\left[\dfrac{\sqrt{(2t)}}{\Delta x}\left(\displaystyle\int_{-\infty}^{-(\zeta-\frac{1}{2}\mu)/\sqrt{(2t)}} \ln\left\{1-F\left(x^2+y-\frac{1}{2t}\left(\zeta-\frac{\mu}{2}\right)^2\right)\right\} dx \right.\right. \\ \quad \left.\left. + \displaystyle\int_{-(\zeta'+\frac{1}{2}\mu')/\sqrt{(2t)}}^{\infty} \ln\left\{1-F\left(x^2+y-\frac{1}{2t}\left(\zeta'+\frac{\mu'}{2}\right)^2\right)\right\} dx\right)\right] dy \\ \qquad\qquad \text{for} \quad \zeta'-\zeta+\tfrac{1}{2}(\mu+\mu') > 0, \\ \quad 0 \qquad\qquad \text{for} \quad \zeta'-\zeta+\tfrac{1}{2}(\mu+\mu') < 0. \end{cases} \tag{5.10}$$

† Here the notation (μ, ζ) stands for a shock whose strength and advance velocity are μ/t and ζ/t respectively.

The factor $$\prod_{i \neq m_1, m_2, m_3} \{1 - F(y_i)\}$$

has been approximated by an integral as before.

When the initial probability distribution $P(y)$ is given by (4.15), the integration in (5.10) for large t can be carried out in just the same way as in the preceding section. Dividing $\tilde{n}_a(\tilde{\mu}, \tilde{\xi}; \tilde{\mu}', \tilde{\xi}'; t)$ thus obtained by the number of shocks per unit length, we get the joint probability distribution for two adjacent shocks:

$$\tilde{g}_a(\tilde{\mu}, \tilde{\xi}; \tilde{\mu}', \tilde{\xi}') = \tilde{n}_a(\tilde{\mu}, \tilde{\xi}; \tilde{\mu}', \tilde{\xi}'; t)/N(t)$$
$$= \begin{cases} \dfrac{\pi^{\frac{7}{2}}}{2^{\frac{1}{2}}} \dfrac{\tilde{\mu}\tilde{\mu}' \exp\{-\pi(\tilde{\mu}\tilde{\xi} - \tilde{\mu}'\tilde{\xi}')\}}{\{\phi(\tilde{\mu} - 2\tilde{\xi}) + \phi(\tilde{\mu}' + 2\tilde{\xi}')\}^3} & \text{for} \quad \tilde{\xi}' - \tilde{\xi} + \dfrac{\tilde{\mu} + \tilde{\mu}'}{2} > 0, \\ 0 & \text{for} \quad \tilde{\xi}' - \tilde{\xi} + \dfrac{\tilde{\mu} + \tilde{\mu}'}{2} < 0, \end{cases} \tag{5.11}$$

where $$\phi(x) = \int_0^\infty \exp(-y^2 + (\tfrac{1}{2}\pi)^{\frac{1}{2}} xy)\, dy. \tag{5.12}$$

If we integrate the joint probability distribution for two adjacent shocks (5.10) or its asymptotic form (5.11) with respect to μ' and ζ' or $\tilde{\mu}'$ and $\tilde{\xi}'$ over the whole region of these variables, we recover the distribution for a single shock (4.13) or (4.33).

All the statistical quantities for two adjacent shocks are derived from (5.11). If (5.11) is integrated with respect to $\tilde{\xi}$ and $\tilde{\xi}'$ under the restraint that their mutual distance

$$\tilde{\lambda} = \tilde{\xi}' - \tilde{\xi} + \tfrac{1}{2}(\tilde{\mu} + \tilde{\mu}') \tag{5.13}$$

is fixed, the joint probability distribution for two adjacent shocks of the strengths $\tilde{\mu}/t$ and $\tilde{\mu}'/t$ separated by the distance $\tilde{\lambda}$ is obtained:

$$\tilde{g}_a(\tilde{\lambda}; \tilde{\mu}, \tilde{\mu}') = \int_{-\infty}^{\infty} d\tilde{\xi} \int_{-\infty}^{\infty} d\tilde{\xi}'\, \tilde{g}_a(\tilde{\mu}, \tilde{\xi}; \tilde{\mu}', \tilde{\xi}')\, \delta(\tilde{\lambda} - \tilde{\xi}' + \tilde{\xi} - \tfrac{1}{2}(\tilde{\mu} + \tilde{\mu}')). \tag{5.14}$$

Further integration of (5.14) with respect to $\tilde{\mu}$ and $\tilde{\mu}'$ yields the distribution for distance between two adjacent shocks

$$\tilde{g}_a(\tilde{\lambda}) = (\tfrac{1}{2}\pi)^{\frac{1}{2}} \frac{d^2}{d\tilde{\lambda}^2} \int_0^\infty \frac{dz}{\phi(\tilde{\lambda} + z) + \phi(\tilde{\lambda} - z)}, \tag{5.15}$$

which has the following asymptotic forms for small and large values of $\tilde{\lambda}$:

$$\tilde{g}_a(\tilde{\lambda}) \approx \sqrt{3} - \tfrac{1}{3}\pi \approx 0{\cdot}685 \quad \text{as} \quad \tilde{\lambda} \to 0, \tag{5.16}$$

$$\tilde{g}_a(\tilde{\lambda}) \approx \frac{(\sqrt{2})\,\pi^2}{32} \tilde{\lambda} \exp(-\tfrac{1}{8}\pi\tilde{\lambda}^2) \quad \text{as} \quad \tilde{\lambda} \to \infty. \tag{5.17}$$

The distribution function $\tilde{g}_a(\tilde{\lambda})$ is depicted together with its asymptotic forms in figure 8.

It can easily be shown that (5.15) satisfies the following integral relations:

$$\int_0^\infty \tilde{g}_a(\tilde{\lambda})\, d\tilde{\lambda} = 1, \tag{5.18}$$

$$\int_0^\infty \tilde{\lambda} \tilde{g}_a(\tilde{\lambda})\, d\tilde{\lambda} = 1. \tag{5.19}$$

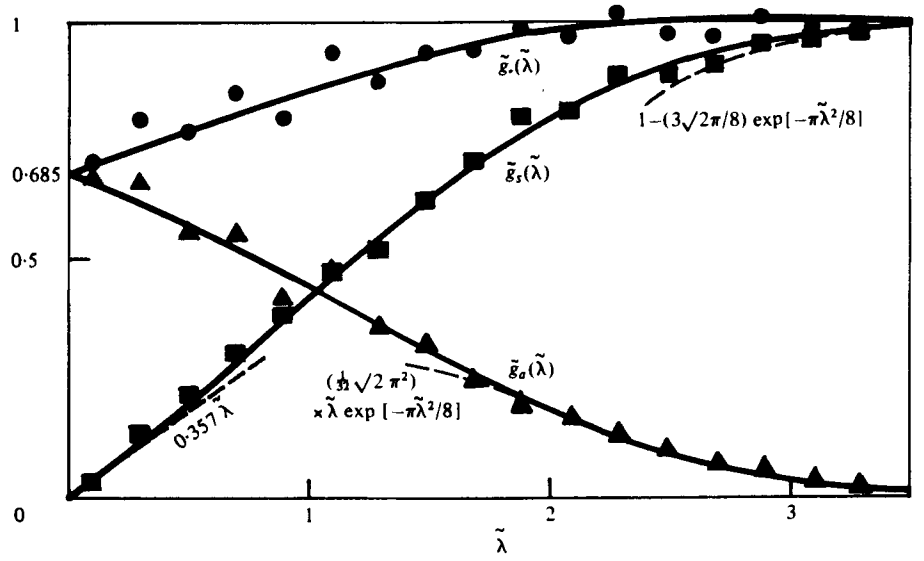

FIGURE 8. The probability distributions for the distance between two shocks in case I. The marks ▲, ■, ● indicate the respective numerical results for the distributions $\tilde{g}_a(\tilde{\lambda})$, $\tilde{g}_s(\tilde{\lambda})$, $\tilde{g}(\tilde{\lambda})$ in experiment (ii).

The relation (5.18) is consistent with the definition of $\tilde{g}_a$ as a probability distribution, while (5.19) shows that the mean value of $\tilde{\lambda}$ is equal to that of $\tilde{\mu}$ [see the first of (4.41)], which is obviously seen from the structure of the velocity field.

It is known that, if the time-dependence of $l(t)$ is assumed to obey the following power law

$$l(t) \propto t^p, \tag{5.20}$$

the exponent p is given by

$$p = \frac{1}{2}\int_0^\infty d\tilde{\mu}\int_0^\infty d\tilde{\mu}'(\tilde{\mu}+\tilde{\mu}')\,\tilde{g}_a(0;\tilde{\mu},\tilde{\mu}') \tag{5.21}$$

(Tatsumi & Kida 1972). A simple calculation using (5.11), (5.12) and (5.14) yields

$$p = \tfrac{1}{2}, \tag{5.22}$$

which coincides with (4.36). Thus the probability distribution functions (4.37) and (5.11) are compatible with (4.36) but not generally with (4.35). This fact may be explained by considering the expression (4.35) as the next-order approximation of $l(t)$. The distribution functions corresponding to it may be obtained by retaining the next-order terms with respect to large t in the integrals of (4.13) and (5.10). By a brief inspection we can see that they are no longer similar functions of t, i.e. they contain the time explicitly.

6. Joint probability distribution for two separated shocks

We now consider two separated shocks. They are represented by a series of contact points which touches each of two parabolas twice and never crosses either of them as illustrated in figure 9.

Let us express the two parabolas by (5.1) and (5.2) and denote the x co-ordinate of their intersection by x. Then the number of the series of contact points which pass

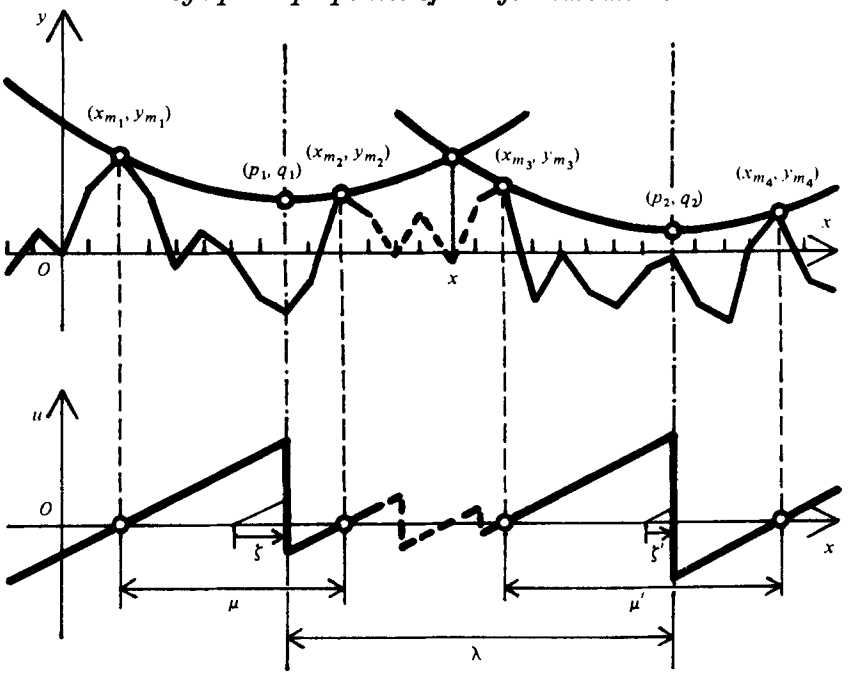

FIGURE 9. A series of contact points representing two separated shocks.

through the areas $dx_{m_1}\,dy_{m_1}$, $dx_{m_2}\,dy_{m_2}$, $dx_{m_3}\,dy_{m_3}$, $dx_{m_4}\,dy_{m_4}$ around the points (x_{m_1}, y_{m_1}), (x_{m_2}, y_{m_2}), (x_{m_3}, y_{m_3}), (x_{m_4}, y_{m_4}) respectively and never cross the two parabolas, where the former two points are on the left parabola and the latter on the right one and

$$x_{m_1} < x_{m_2} < x_{m_3} < x_{m_4},$$

is given by

$$\frac{1}{(\Delta x)^4}\prod_{j=1}^{4} P(y_{m_j})\,dx_{m_j}\,dy_{m_j}\prod_{i\neq m_1,\,m_2,\,m_3,\,m_4,}\{1-F(y_i)\}, \tag{6.1}$$

where

$$y_i = \begin{cases} \dfrac{1}{2t}(x_i-p_1)^2+q_1 & \text{for} \quad x_i \leqslant x, \\ \dfrac{1}{2t}(x_i-p_2)^2+q_2 & \text{for} \quad x_i > x. \end{cases} \tag{6.2}$$

Denote the shocks located at p_1 and p_2 by (μ, ζ) and (μ', ζ') respectively. Then we have the following relations:

$$\mu = x_{m_2}-x_{m_1}, \quad \mu' = x_{m_4}-x_{m_3}, \tag{6.3}$$

$$\frac{\mu\zeta}{t} = y_{m_1}-y_{m_2}, \quad \frac{\mu'\zeta'}{t} = y_{m_3}-y_{m_4}, \tag{6.4}$$

$$p_1 = x_{m_2}+\zeta-\frac{\mu}{2}, \quad p_2 = x_{m_3}+\zeta'+\frac{\mu'}{2}, \tag{6.5}$$

$$q_1 = y_{m_2}-\frac{1}{2t}\left(\zeta-\frac{\mu}{2}\right)^2, \quad q_2 = y_{m_3}-\frac{1}{2t}\left(\zeta'+\frac{\mu'}{2}\right)^2, \tag{6.6}$$

$$x = \tfrac{1}{2}(p_1+p_2)+\frac{q_2-q_1}{p_2-p_1}t. \tag{6.7}$$

The distance between the two shocks is written as

$$\lambda = p_2 - p_1 = x_{m_3} - x_{m_2} + \zeta' - \zeta + \frac{\mu+\mu'}{2}, \tag{6.8}$$

where (6.5) has been used.

In order that such a pair of shocks exist the following relation must be satisfied:

$$x_{m_2} < x < x_{m_3}, \tag{6.9}$$

as clearly seen from figure 9. The condition (6.9) is rewritten as

$$-\frac{\lambda}{t}(\tfrac{1}{2}\lambda + \zeta - \tfrac{1}{2}\mu) < q_2 - q_1 < \frac{\lambda}{t}(\tfrac{1}{2}\lambda - \zeta' - \tfrac{1}{2}\mu'), \tag{6.10}$$

using (6.3)–(6.8), which demands

$$\lambda > \zeta' - \zeta + \frac{\mu+\mu'}{2} \tag{6.11}$$

as a necessary condition.

By transforming the variables in (6.1) from x_{mj}, y_{mj}, $j = 1, 2, 3, 4$ into $\lambda, \mu, \zeta, \mu', \zeta'$, q_1, q_2, x through (6.3)–(6.8), we get the number density for two separated shocks (μ, ζ) and (μ', ζ') with the distance λ as follows:

$$\begin{aligned} &n_s(\lambda;\mu,\zeta;\mu',\zeta';t) \\ &= \frac{1}{(\Delta x)^4}\frac{\mu\mu'}{t^2}\iint_D dq_1\,dq_2 \frac{P\left(q_1+\frac{1}{2t}(\zeta+\frac{1}{2}\mu)^2\right)}{1-F\left(q_1+\frac{1}{2t}(\zeta+\frac{1}{2}\mu)^2\right)}\frac{P\left(q_1+\frac{1}{2t}(\zeta-\frac{1}{2}\mu)^2\right)}{1-F\left(q_1+\frac{1}{2t}(\zeta-\frac{1}{2}\mu)^2\right)} \\ &\times \frac{P\left(q_2+\frac{1}{2t}(\zeta'+\frac{1}{2}\mu')^2\right)}{1-F\left(q_2+\frac{1}{2t}(\zeta'+\frac{1}{2}\mu')^2\right)}\frac{P\left(q_2+\frac{1}{2t}(\zeta'-\frac{1}{2}\mu')^2\right)}{1-F\left(q_2+\frac{1}{2t}(\zeta'-\frac{1}{2}\mu')^2\right)} \\ &\times \exp\left[\frac{(2t)^{\frac{1}{2}}}{\Delta x}\left(\int_{-\infty}^{(\frac{1}{2}\lambda+(q_2-q_1)t/\lambda)/\sqrt{(2t)}} \ln\{1-F(x^2+q_1)\}\,dx\right.\right. \\ &\left.\left.+\int_{-(\frac{1}{2}\lambda-(q_2-q_1)t/\lambda)/\sqrt{(2t)}}^{\infty} \ln\{1-F(x^2+q_2)\}\,dx\right)\right], \end{aligned} \tag{6.12}$$

where D denotes that the integration with respect to q_1 and q_2 should be carried out under the condition (6.10). The factor

$$\prod_{i\neq m_1, m_2, m_3, m_4} \{1-F(y_i)\}$$

in (6.1) has been replaced by an integral as before. The integration in (6.12) for large t can be performed by the method of steepest descent as in the preceding sections when $P(y)$ is given by (4.15). Dividing $\tilde{n}_s(\tilde{\lambda};\tilde{\mu},\tilde{\zeta};\tilde{\mu}',\tilde{\zeta}';t)$ thus calculated by $N(t)$, we get the joint probability distribution function for two separated shocks $(\tilde{\mu},\tilde{\zeta})$ and $(\tilde{\mu}',\tilde{\zeta}')$ with the distance $l(t)\tilde{\lambda}$:

$$\tilde{g}_s(\tilde{\lambda};\tilde{\mu},\tilde{\zeta};\tilde{\mu}',\tilde{\zeta}') = \begin{cases} \frac{3}{2}\pi^5\tilde{\lambda}\tilde{\mu}\tilde{\mu}'\exp\{-\pi(\frac{1}{4}\tilde{\mu}^2+\frac{1}{4}\tilde{\mu}'^2+\tilde{\zeta}^2+\tilde{\zeta}'^2-\frac{1}{2}\tilde{\lambda}^2)\} \\ \quad\times\int_{\frac{1}{2}\tilde{\lambda}-\tilde{\zeta}+\frac{1}{2}\tilde{\mu}}^{\frac{1}{2}\tilde{\lambda}-\tilde{\zeta}'-\frac{1}{2}\tilde{\mu}'} \dfrac{\exp(2\pi s^2)}{\{\phi(\tilde{\lambda}+2s)+\phi(\tilde{\lambda}-2s)\}^4}ds \quad \text{for} \quad \tilde{\lambda} > \tilde{\zeta}'-\tilde{\zeta}+\dfrac{\tilde{\mu}+\tilde{\mu}'}{2}, \\ 0 \quad \text{for} \quad \tilde{\lambda} < \tilde{\zeta}'-\tilde{\zeta}+\dfrac{\tilde{\mu}+\tilde{\mu}'}{2}, \end{cases} \tag{6.13}$$

which has the following asymptotic form:

$$\tilde{g}_s(\tilde{\lambda};\tilde{\mu},\tilde{\xi};\tilde{\mu}',\tilde{\xi}') \approx \tilde{f}(\tilde{\mu},\tilde{\xi})\tilde{f}(\tilde{\mu}',\tilde{\xi}') \quad \text{as} \quad \tilde{\lambda}\to\infty, \tag{6.14}$$

where the neglected terms are exponentially small. This indicates that the distributions for any pair of shocks become independent of each other sufficiently rapidly as their mutual distance increases. As $\tilde{\lambda}$ goes to zero, on the other hand, (6.13) for

$$\tilde{\xi}-\tilde{\xi}'-\tfrac{1}{2}(\tilde{\mu}+\tilde{\mu}') > 0$$

becomes

$$\tilde{g}_s(\tilde{\lambda};\tilde{\mu},\tilde{\xi};\tilde{\mu}',\tilde{\xi}') \approx \frac{3\pi^3}{2}\tilde{\lambda}\tilde{\mu}\tilde{\mu}'\left(\tilde{\xi}-\tilde{\xi}'-\frac{\tilde{\mu}+\tilde{\mu}'}{2}\right)\exp\left\{-\pi\left(\frac{\tilde{\mu}^2}{4}+\frac{\tilde{\mu}'^2}{4}+\tilde{\xi}^2+\tilde{\xi}'^2\right)\right\}, \tag{6.15}$$

i.e. $\tilde{g}_s$ vanishes in proportion to $\tilde{\lambda}$.

By integrating (6.13) with respect to $\tilde{\xi}$ and $\tilde{\xi}'$ from $-\infty$ to ∞, we obtain the joint probability distribution for two separated shocks of strengths $l(t)\,\tilde{\mu}/t$ and $l(t)\,\tilde{\mu}'/t$ with the distance $l(t)\,\tilde{\lambda}$:

$$\tilde{g}_s(\tilde{\lambda};\tilde{\mu},\tilde{\mu}') = \int_{-\infty}^{\infty} d\tilde{\xi}\int_{-\infty}^{\infty} d\tilde{\xi}'\,\tilde{g}_s(\tilde{\lambda};\tilde{\mu},\tilde{\xi};\tilde{\mu}',\tilde{\xi}'). \tag{6.16}$$

Further integration of (6.16) with respect to $\tilde{\mu}$ and $\tilde{\mu}'$ in the domain $[0,\infty)$ leads to the probability for existence of two separated shocks with the distance $l(t)\,\tilde{\lambda}$ irrespective of their strengths and advance velocities:

$$\tilde{g}_s(\tilde{\lambda}) = \int_0^{\infty} d\tilde{\mu}\int_0^{\infty} d\tilde{\mu}'\tilde{g}_s(\tilde{\lambda};\tilde{\mu},\tilde{\mu}'). \tag{6.17}$$

Substituting (6.13) and (6.16) into (6.17), we find that

$$\tilde{g}_s(\tilde{\lambda}) = 3\pi^2\tilde{\lambda}\int_0^{\infty}\frac{\{\sqrt{2}\,\phi(\sqrt{2}\,(\tilde{\lambda}+s))-\phi(\tilde{\lambda}+s)\}\{\sqrt{2}\,\phi(\sqrt{2}\,(\tilde{\lambda}-s))-\phi(\tilde{\lambda}-s)\}}{\{\phi(\tilde{\lambda}+s)+\phi(\tilde{\lambda}-s)\}^4}ds. \tag{6.18}$$

This distribution function has the following asymptotic forms for small and large values of $\tilde{\lambda}$:

$$\tilde{g}_s(\tilde{\lambda}) \approx \frac{3\sqrt{2}}{4}\left(4-\frac{3\sqrt{2}}{2}\pi+4\sqrt{2}\arctan\frac{\sqrt{2}}{2}-\sqrt{2}\arctan\frac{\sqrt{2}}{4}\right)\tilde{\lambda}$$
$$\approx 0{\cdot}357\tilde{\lambda} \qquad \text{as} \quad \tilde{\lambda}\to 0, \tag{6.19}$$

$$\tilde{g}_s(\tilde{\lambda}) \approx 1-\frac{3\sqrt{(2)}\pi}{8}\exp\left(-\frac{\pi\tilde{\lambda}^2}{8}\right) \quad \text{as} \quad \tilde{\lambda}\to\infty. \tag{6.20}$$

This tells us that $\tilde{g}_s(\tilde{\lambda})$ tends to 1 at infinity, which implies that far-off shocks are scattered independent of each other at the rate of one shock per mean distance $l(t)$.

The sum of (5.15) and (6.18) gives the probability for existence of any two shocks separated by $l(t)\,\tilde{\lambda}$:

$$\tilde{g}(\tilde{\lambda}) = \tilde{g}_a(\tilde{\lambda})+\tilde{g}_s(\tilde{\lambda}). \tag{6.21}$$

The functions (6.18) and (6.21) are depicted together with their asymptotic forms in figure 8. It may be observed that $\tilde{g}(\tilde{\lambda})$ for small $\tilde{\lambda}$ are smaller than that for large $\tilde{\lambda}$. This reflects the fact that a pair of shocks which are close together are more likely to be destroyed by collision than that of widely separated shocks.

7. Velocity correlation and energy spectrum

Now that the joint probability distribution function $g(r;\mu,\mu';t)$ for the strength of any two shocks separated by the distance r is known, we can calculate the velocity correlation function $B(r,t)$ defined by (3.1). As shown in § 2, the velocity field for $R \gg t \gg 1$ is composed of a series of vertical lines (shocks) spaced alternately with oblique lines of slope $1/t$. The space derivative of velocity $u'(x,t)$ is given by

$$-(\mu/t)\delta(x-\xi)$$

at a shock, where ξ and μ/t are the position and the strength of the shock, and by $1/t$ in the region of oblique lines. Therefore we have

$$\left\langle \left(u'(x,t)-\frac{1}{t}\right)\left(u'(x+r,t)-\frac{1}{t}\right)\right\rangle = \frac{1}{t^2 l(t)}\int_0^\infty d\mu \int_0^\infty d\mu' \mu\mu' g(r;\mu,\mu';t). \tag{7.1}$$

Since $\langle u'(x,t)\rangle = 0$, the left-hand side is rewritten as

$$\langle u'(x,t)\,u'(x+r,t)\rangle + \frac{1}{t^2} = -\frac{\partial^2}{\partial r^2}B(r,t) + \frac{1}{t^2} = -\frac{1}{t^2}\left\{\frac{d^2}{d\tilde{r}^2}\tilde{B}(\tilde{r}) - 1\right\}, \tag{7.2}$$

where

$$\tilde{B}(\tilde{r}) = \left(\frac{t}{l(t)}\right)^2 B(r,t).\dagger \tag{7.3}$$

The right-hand side, on the other hand, is replaced by

$$\frac{1}{t^2\langle\tilde{\mu}\rangle}\int_0^\infty d\tilde{\mu}\int_0^\infty d\tilde{\mu}'\tilde{\mu}\tilde{\mu}'\tilde{g}(\tilde{r};\tilde{\mu},\tilde{\mu}'). \tag{7.4}$$

Therefore (7.1) leads to

$$\frac{d^2}{d\tilde{r}^2}\tilde{B}(\tilde{r}) = 1 - \frac{1}{\langle\tilde{\mu}\rangle}\int_0^\infty d\tilde{\mu}\int_0^\infty d\tilde{\mu}'\tilde{\mu}\tilde{\mu}'\tilde{g}(\tilde{r};\tilde{\mu},\tilde{\mu}'). \tag{7.5}$$

Integrating (7.5) twice with respect to $\tilde{r}$ under the conditions

$$\tilde{B}(\tilde{r}) = \frac{d}{d\tilde{r}}\tilde{B}(\tilde{r}) = 0 \quad \text{at} \quad \tilde{r}\to\infty, \tag{7.6}$$

we obtain

$$\tilde{B}(\tilde{r}) = \int_{\tilde{r}}^\infty (\tilde{r}'-\tilde{r})\left\{1 - \frac{1}{\langle\tilde{\mu}\rangle}\int_0^\infty d\tilde{\mu}\int_0^\infty d\tilde{\mu}'\tilde{\mu}\tilde{\mu}'\tilde{g}(\tilde{r}';\tilde{\mu},\tilde{\mu}')\right\}d\tilde{r}'. \tag{7.7}$$

Another equivalent expression of $\tilde{B}(\tilde{r})$ has been derived by Burgers (1950):

$$\tilde{B}(\tilde{r}) = \frac{1}{\langle\tilde{\mu}\rangle}\left\{\langle\tilde{\mu}\tilde{\xi}^2\rangle + \tfrac{1}{12}\langle\tilde{\mu}^3\rangle - \frac{\langle\tilde{\mu}^2\rangle}{2}\tilde{r} + \frac{\langle\tilde{\mu}\rangle}{2}\tilde{r}^2 - \int_0^{\tilde{r}} d\tilde{r}'(\tilde{r}-\tilde{r}')\int_0^\infty d\tilde{\mu}\int_0^\infty d\tilde{\mu}'\tilde{\mu}\tilde{\mu}'\tilde{g}(\tilde{r}';\tilde{\mu},\tilde{\mu}')\right\}. \tag{7.8}$$

The expression (7.7) is convenient for investigating the behaviour of $\tilde{B}(\tilde{r})$ for large $\tilde{r}$, while (7.8) is useful for small $\tilde{r}$. It follows from (7.8) that

$$\tilde{B}'(0+) \equiv \left[\frac{d\tilde{B}(\tilde{r})}{d\tilde{r}}\right]_{\tilde{r}\to 0+} = -\frac{\langle\tilde{\mu}^2\rangle}{2\langle\tilde{\mu}\rangle}(\neq 0). \tag{7.9}$$

This reflects the discontinuous structure of the velocity field under the condition $R \gg t \gg 1$.

† In §8.2 the velocity correlation function will be normalized with reference to J and t in order to compare with results due to Burgers (1974) [(see 8.13)].

Let us define the turbulent energy per unit length by

$$\mathscr{E}(t) = \tfrac{1}{2}\langle u(x,t)^2\rangle = \tfrac{1}{2}B(0,t), \tag{7.10}$$

where the fluid is assumed to have unit density. By making use of (7.3), (7.8) and (4.40), we can rewrite (7.10) as

$$\mathscr{E}(t) = \frac{1}{2}\left(\frac{l(t)}{t}\right)^2 \frac{1}{\langle\tilde{\mu}\rangle}(\langle\tilde{\mu}\tilde{\zeta}^2\rangle + \tfrac{1}{12}\langle\tilde{\mu}^3\rangle) = \frac{1}{2\pi}\left(\frac{l(t)}{t}\right)^2. \tag{7.11}$$

Since $l(t)$ for large t is expressed by (4.36), we find that

$$\mathscr{E}(t) \propto 1/t. \tag{7.12}$$

This is the energy decay law in the case $J = 0$.

In order to work out the form of $\tilde{B}(\tilde{r})$ explicitly, we must calculate the integral

$$\int_0^\infty d\tilde{\mu}\int_0^\infty d\tilde{\mu}'\tilde{\mu}\tilde{\mu}'\tilde{g}(\tilde{r};\tilde{\mu},\tilde{\mu}') = \int_0^\infty d\tilde{\mu}\int_0^\infty d\tilde{\mu}'\tilde{\mu}\tilde{\mu}'\tilde{g}_a(\tilde{r};\tilde{\mu},\tilde{\mu}') + \int_0^\infty d\tilde{\mu}\int_0^\infty d\tilde{\mu}'\tilde{\mu}\tilde{\mu}'\tilde{g}_s(\tilde{r};\tilde{\mu},\tilde{\mu}'). \tag{7.13}$$

The first term on the right-hand side is converted, using (5.11) and (5.14), into

$$\int_0^\infty d\tilde{\mu}\int_0^\infty d\tilde{\mu}'\tilde{\mu}\tilde{\mu}'\tilde{g}_a(\tilde{r};\tilde{\mu},\tilde{\mu}') = \frac{16\sqrt{2}}{\pi^{\frac{1}{2}}}\int_0^\infty \frac{\phi''(\tilde{r}+s)\,\phi''(\tilde{r}-s)}{\{\phi(\tilde{r}+s)+\phi(\tilde{r}-s)\}^3}\,ds \tag{7.14}$$

and the second, using (6.13) and (6.16), into

$$\int_0^\infty d\tilde{\mu}\int_0^\infty d\tilde{\mu}'\tilde{\mu}\tilde{\mu}'\tilde{g}_s(\tilde{r};\tilde{\mu},\tilde{\mu}') = \tfrac{3}{2}\pi\tilde{r}\int_0^\infty \frac{\{2\phi(\tilde{r}+s)^2-\phi'(\tilde{r}+s)\}\{2\phi(\tilde{r}-s)^2-\phi'(\tilde{r}-s)\}}{\{\phi(\tilde{r}+s)+\phi(\tilde{r}-s)\}^4}\,ds. \tag{7.15}$$

Then $\tilde{B}(\tilde{r})$ is obtained by putting (7.13)–(7.15) into (7.7) or (7.8) as follows:

$$\tilde{B}(\tilde{r}) = \frac{1}{\sqrt{(2\pi)}}\frac{d}{d\tilde{r}}\tilde{r}\int_0^\infty \frac{ds}{\phi(\tilde{r}+s)+\phi(\tilde{r}-s)}, \tag{7.16}$$

which has the following asymptotic forms:

$$\tilde{B}(\tilde{r}) \approx \frac{1}{\pi} - \frac{2}{\pi}\tilde{r} \qquad \text{as} \quad \tilde{r}\to 0, \tag{7.17}$$

$$\tilde{B}(\tilde{r}) \approx -\frac{\sqrt{2}}{8}\tilde{r}\exp\left(-\frac{\pi\tilde{r}^2}{8}\right) \qquad \text{as} \quad \tilde{r}\to\infty. \tag{7.18}$$

The velocity correlation function (7.16) is depicted together with its asymptotic forms in figure 10. It starts with a positive value at $\tilde{r} = 0$, decreases linearly with $\tilde{r}$ at first, becomes negative, takes a minimum value and finally approaches zero exponentially.

The energy spectrum function is defined by Fourier transformation of the velocity correlation function:

$$E(k,t) = \frac{1}{\pi}\int_0^\infty B(r,t)\cos kr\,dr. \tag{7.19}$$

Integration of $E(k,t)$ with respect to k from 0 to ∞ gives the turbulent energy per unit length

$$\mathscr{E}(t) = \int_0^\infty E(k,t)\,dk, \tag{7.20}$$

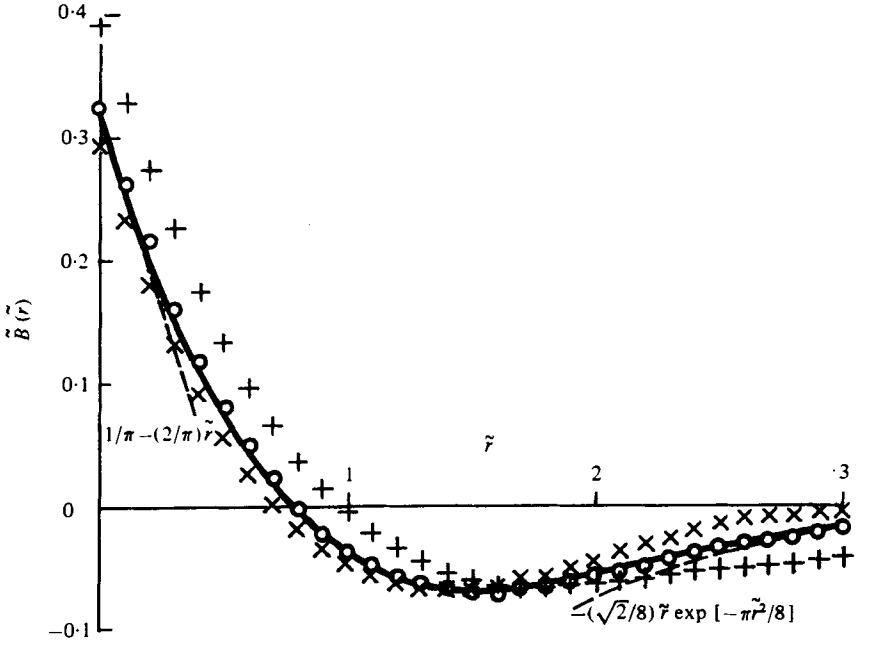

FIGURE 10. The velocity correlation function for case I.

which has already been calculated above [see (7.10)–(7.12)]. In terms of the normalized wavenumber

$$\tilde{k} = l(t)\,k, \tag{7.21}$$

and the normalized energy spectrum

$$\tilde{E}(\tilde{k}) = \frac{t^2}{l(t)^3} E(k,t), \tag{7.22}$$

the energy spectrum function (7.19) is expressed as

$$\tilde{E}(\tilde{k}) = \frac{1}{\pi}\int_0^\infty \tilde{B}(\tilde{r})\cos\tilde{k}\tilde{r}\,d\tilde{r}. \tag{7.23}$$

Substituting (7.16) into (7.23), we get

$$\tilde{E}(\tilde{k}) = \frac{\tilde{k}}{\sqrt{(2\pi^3)}}\int_0^\infty dr\,r\sin\tilde{k}r\int_0^\infty \frac{ds}{\phi(r+s)+\phi(r-s)}, \tag{7.24}$$

which has the following asymptotic forms:

$$\tilde{E}(\tilde{k}) \approx \frac{\tilde{k}^2}{\sqrt{(2\pi^3)}}\int_0^\infty dr\,r^2\int_0^\infty \frac{ds}{\phi(r+s)+\phi(r-s)} \approx 0{\cdot}062\tilde{k}^2 \quad \text{for small } \tilde{k}, \tag{7.25}$$

$$\tilde{E}(\tilde{k}) \approx \frac{2}{\pi^2}\tilde{k}^{-2} \quad \text{for large } \tilde{k}. \tag{7.26}$$

The energy spectrum function (7.24) and its asymptotic forms (7.25) and (7.26) are shown graphically in figure 11. Kolmogorov's $k^{-\frac{5}{3}}$ energy spectrum is not observed here.

The behaviour of $\tilde{E}(\tilde{k})$ for small $\tilde{k}$ is examined by expanding $\cos\tilde{k}\tilde{r}$ in (7.23) in powers of $\tilde{k}$:

$$\tilde{E}(\tilde{k}) = \frac{1}{\pi}\int_0^\infty \tilde{B}(\tilde{r})\,d\tilde{r} - \frac{\tilde{k}^2}{2\pi}\int_0^\infty \tilde{r}^2\tilde{B}(\tilde{r})\,d\tilde{r} + \ldots. \tag{7.27}$$

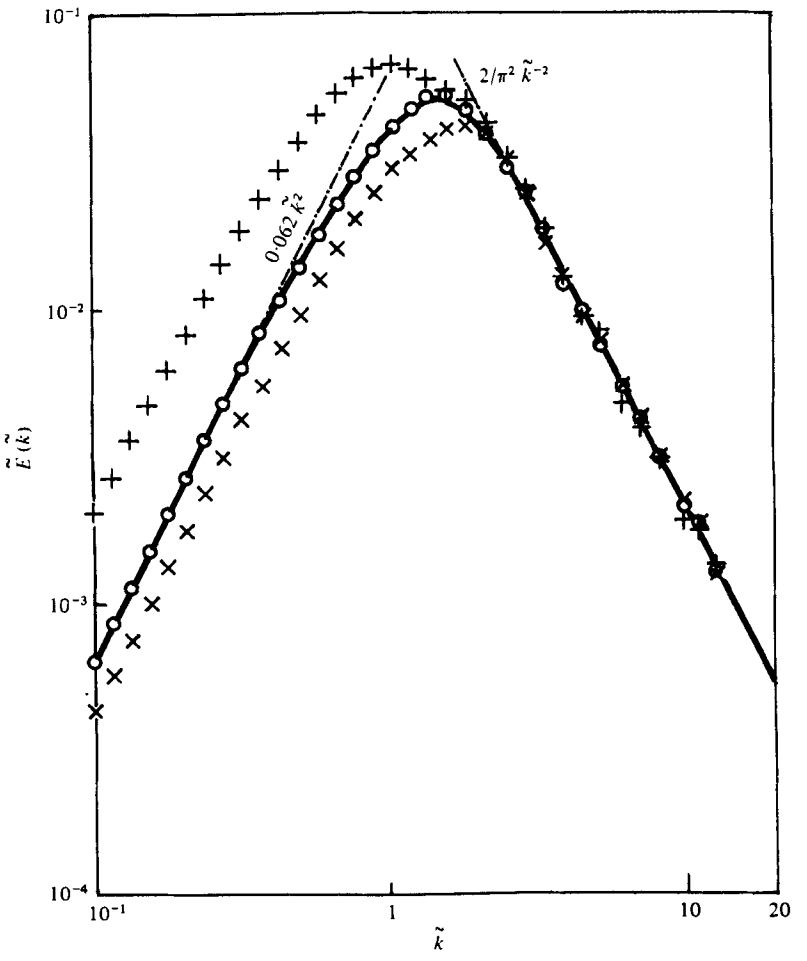

FIGURE 11. The energy spectrum function for case I.

Comparing it with (7.25), we find

$$J = \frac{l(t)^3}{t^2}\int_0^\infty \tilde{B}(\tilde{r})\,d\tilde{r} = 0. \tag{7.28}$$

This result confirms that the initial distribution (4.15) actually produces a velocity field which satisfies the condition $J = 0$.

The asymptotic behaviour of $\tilde{E}(\tilde{k})$ for large values of $\tilde{k}$, on the other hand, is examined by integrating (7.23) by part:

$$\tilde{E}(\tilde{k}) = -\frac{\tilde{B}'(0+)}{\pi}\tilde{k}^{-2} + O(\tilde{k}^{-4}) = \frac{\langle\tilde{\mu}^2\rangle}{2\pi\langle\tilde{\mu}\rangle}\tilde{k}^{-2} + O(\tilde{k}^{-4}), \tag{7.29}$$

where (7.9) has been used. Since $\tilde{B}'(0+) = -2/\pi$ from (7.17), the asymptotic form (7.29) coincides with (7.26). The $\tilde{k}^{-2}$ dependence of the energy spectrum function in the region of large values of wavenumber results from the discontinuous structure of the velocity field, in which $\tilde{B}'(0+) \neq 0$. If the velocity field were continuous, then we might have $\tilde{B}'(0) = 0$ and $\tilde{E}(\tilde{k}) \sim O(\tilde{k}^{-4})$ for large values of $\tilde{k}$. It should be noted that when the

velocity field $u(x,t)$ is infinitely differentiable with respect to x, then the energy spectrum falls to zero faster than any negative power of the wavenumber as it goes to infinity.

8. Numerical experiments

Now we shall investigate numerically how the velocity field develops after it starts with a random initial condition. Since we are interested in the situation $R \gg t \gg 1$, the velocity field is expressed as a system of shocks and oblique lines. Instead of integrating the Burgers equation of motion directly we construct the solutions with the aid of a procedure using the parabolas and the s curves. For carrying out numerical experiments it seems more convenient to use the description of the system due to Tatsumi & Kida (1972) than that due to Burgers (1974) which has been used in the preceding sections. Although the parabolas and the s curves are employed in different ways, these two are equivalent.

Denote the tops of the s curve by (x_i, y_i), where i are integers and $x_i < x_{i'}$ for $i < i'$. To each top (x_i, y_i) we attach a parabola which opens *downward*† and the vertex of which is on it:

$$y = -(x-x_i)^2/2t + y_i. \tag{8.1}$$

We take the highest parabolic arc at each point of x. The set of these arcs represents the velocity field completely. It can be easily shown that the vertices of parabolic arcs and the intersections of adjacent arcs give the intersections of oblique lines with the x axis and the positions of shocks respectively. Note that the above relation between parabolas and shocks is the reverse of that in Burgers' procedure. Statistics of the highest parabolic arcs determines all statistical quantities for shocks such as the probability distributions for μ, ζ and λ, the velocity correlation function and the energy spectrum function.

The set of highest parabolic arcs at any instant is determined successively by that at a previous instant. Let $\{x_i\}$ and $\{x_i'\}$ be the sets of the x co-ordinates of the vertices of the highest parabolic arcs at t and t' $(t < t')$ respectively and let ξ_i be the x co-ordinate of the intersection of two adjacent parabolas attached to x_i and x_{i+1} at t'. Then the set $\{\xi_i\}$ represents the positions of shocks at t'. Select from $\{\xi_i\}$ the elements which satisfy the condition $\xi_i < \xi_{i'}$ for $i < i'$ and denote them by $\{\xi_i'\}$. Then the set $\{x_i'\}$ is composed of the elements in $\{x_i\}$ which contribute to yield $\{\xi_i'\}$. Since $\{x_i'\}$ is a subset of $\{x_i\}$, the number of the elements in the former is fewer than that in the latter. This implies a decrease in number of shocks, which arises from coalescence of shocks by collision. In this way the set of highest parabolic arcs at t' is determined by that at a previous instant t. This process is repeated at every time step in numerical experiments.

The above argument makes it possible to give the set of highest parabolic arcs at any time, say t_1, when shocks and oblique lines are already formed instead of at the initial instant. We can choose as this time the one at which the typical length is much longer than that at the initial instant but much shorter than that at times which we are now considering. For simplicity of description we use the length- and time-scales referred to a state at a time under consideration, not to the initial state. In practice, in case I we

† We reverse the y-axis in the original paper in order to get the identical configuration of shocks as in the present paper.

Experiment	$P(y)$	$\Delta x A$	B
(i)	$\Delta x A \exp[-B\|y\|^{\frac{1}{2}}]$	$\frac{1}{4}B^2$	5·72588
(ii)	$\Delta x A \exp[-B\|y\|]$	$\frac{1}{2}\pi$	π
(iii)	$\Delta x A \exp[-By^2]$	$(B/\pi)^{\frac{1}{2}}$	0·975587

TABLE 1. The probability for the y co-ordinates of vertices of the highest parabolic arcs given at t_{I}.

put the mean distance between two adjacent shocks $l(t)$ at unit at $t = 1$, while in case II we put the integral scale of the velocity correlation function J at unit in order to get the same length-scale of the velocity field as that used by Burgers (1974).

The numerical experiments are made in a finite domain $\mathscr{D}$. The x axis is divided by the discrete points specified by (4.1), where $\Delta x \ll 1$. The vertices of the highest parabolic arcs at t_{I} are assigned on these points. This restriction is permissible so long as we deal with the situation at $t \gg t_{\mathrm{I}}$, in which the typical length is much longer than Δx, i.e. $l(t) \gg \Delta x$.

Two cases $J = 0$ and $J \neq 0$ will be studied in §§ 8.1 and 8.2, respectively. The former has the intention of comparing with the results obtained analytically in the present paper and the latter with the predictions by Burgers (1974).

8.1. *Case* I: $J = 0$

The y co-ordinates of vertices of the highest parabolic arcs at t_{I} are given on the points (4.1) independently of each other by random numbers produced by a computer with a prescribed probability $P(y)$. They are given in a sufficiently large domain over $\mathscr{D}$ so as to make the velocity field in $\mathscr{D}$ homogeneous. We make three experiments with the probabilities (i) $P(y) = \Delta x A \exp[-B|y|^{\frac{1}{2}}]$, (ii) $P(y) = \Delta x A \exp[-B|y|]$ and (iii) $P(y) = \Delta x A \exp[-By^2]$, which have the asymptotes of the type (4.15) with $\alpha = 0$ and $\beta = \frac{1}{2}$, 1, 2, respectively. The step Δx is always set at 0·01. The constants A and B are so chosen that the condition (4.2) holds and that $l(t)$ calculated from (4.24) and (4.28) satisfies the condition $l(1) = 1$. Their values are listed in table 1. The length of the domain $\mathscr{D}$ is determined in order that it contains ten thousand of shocks at $t = 1$. The highest parabolic arcs are determined successively at $t = 2^n$, $n = 0, 1, 2, \ldots, 10$.

Total number of shocks contained in $\mathscr{D}$, which is equal to that of the highest parabolic arcs, is counted at every time. Dividing it by the length of $\mathscr{D}$, we obtain $N(t)$ and its reciprocal $l(t)$. They are plotted in figure 12 together with the analytical curves derived from (4.24) and (4.28). It is seen that the analytical and experimental results for experiment (ii) are in perfect agreement. For (i) or (iii), however, they diverge by about 20 or 10% respectively, while their time-dependences are in good agreement. This disagreement may come from the errors included in the approximate estimations (e.g. (4.21)–(4.23)) made in § 4. In fact, $\bar{q}(t)$ is 0·83–3·05 or 1·61–2·42 in (i) or (iii) respectively, which is not sufficiently small and gives rise to the above magnitudes of errors. Incidentally it should be noted that the curves for (i) and (iii) are not straight but bend in the direction of the line for (ii). This suggests that the typical length in the numerical experiments with $\Delta x \ll 0{\cdot}01$ would become such as to satisfy (4.36).

The distribution functions for the strength and the advance velocity of a single shock and for the distance between two shocks, the velocity correlation function and

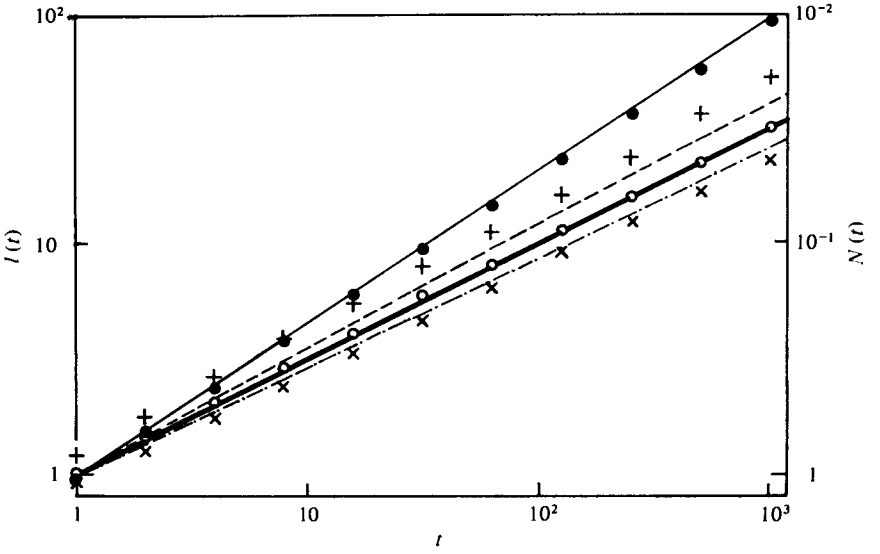

FIGURE 12. The time-dependences of the characteristic length and the number density of shocks. The curves - - -, ——, – · – · – indicate respectively those for experiments (i), (ii) and (iii) in case I The line —— and the mark ● indicate the analytical and experimental results in case II.

the energy spectrum function are calculated from the positions of vertices of the highest parabolic arcs at every time step. It is found that all the above functions have self-preserving forms with respect to time, which has already been predicted analytically. That is, when the length-scale is normalized with reference to $l(t)$, the values of the functions obtained numerically coincide with each other at different times. Therefore we shall show below only the data at $t = 1$ as the representative ones.

The distributions for the strength and the advance velocity of a single shock are obtained as follows. The $\tilde{\mu}$, $\tilde{\zeta}$ plane is divided into square meshes of sides of 0·2. The number of shocks whose strength and advance velocity are included in each mesh is counted. Dividing them by the total number of shocks we obtain the joint probability distribution for the strength and the advance velocity of a single shock. It turns out that the relation (4.37) holds perfectly in experiment (ii) and approximately in (i) and (iii), that is, the distributions for $\tilde{\mu}$ and $\tilde{\zeta}$ are independent of each other. The distribution for a single variable $\tilde{\mu}$ or $\tilde{\zeta}$ is obtained from the partial sums of the joint probability distribution. Those at $t = 1$ are plotted in figures 5 and 6, respectively. They are again in good agreement with the analytical curves in experiment (ii), but a slight discrepancy is observed in (i) and (iii).

The distributions for the distance $\tilde{\lambda}$ between two shocks are obtained by counting the number of pairs of such shocks that $0{\cdot}2(n-1) < \tilde{\lambda} \leqslant 0{\cdot}2n$, $n = 1, 2, \ldots$. Those of adjacent shocks and separated shocks, and their sum at $t = 1$ for experiment (ii) are plotted in figure 8. The agreement with the analytical curves is quite satisfactory though there are some fluctuations in the data. For experiments (i) and (iii), the data of which are omitted here, it is observed that those at small $\tilde{\lambda}(\lesssim 1)$ are higher and lower by several per cent than the analytical curves respectively, but both of them at large $\tilde{\lambda}(\gtrsim 1)$ agree well with the analytical curves.

The turbulent energy per unit length $\mathscr{E}(t)$ is calculated from (7.11), where $l(t)\,(=\langle\tilde{\mu}\rangle)$, $\langle\tilde{\mu}\tilde{\zeta}^2\rangle$ and $\langle\tilde{\mu}^3\rangle$ are determined numerically. The results are plotted in figure 13

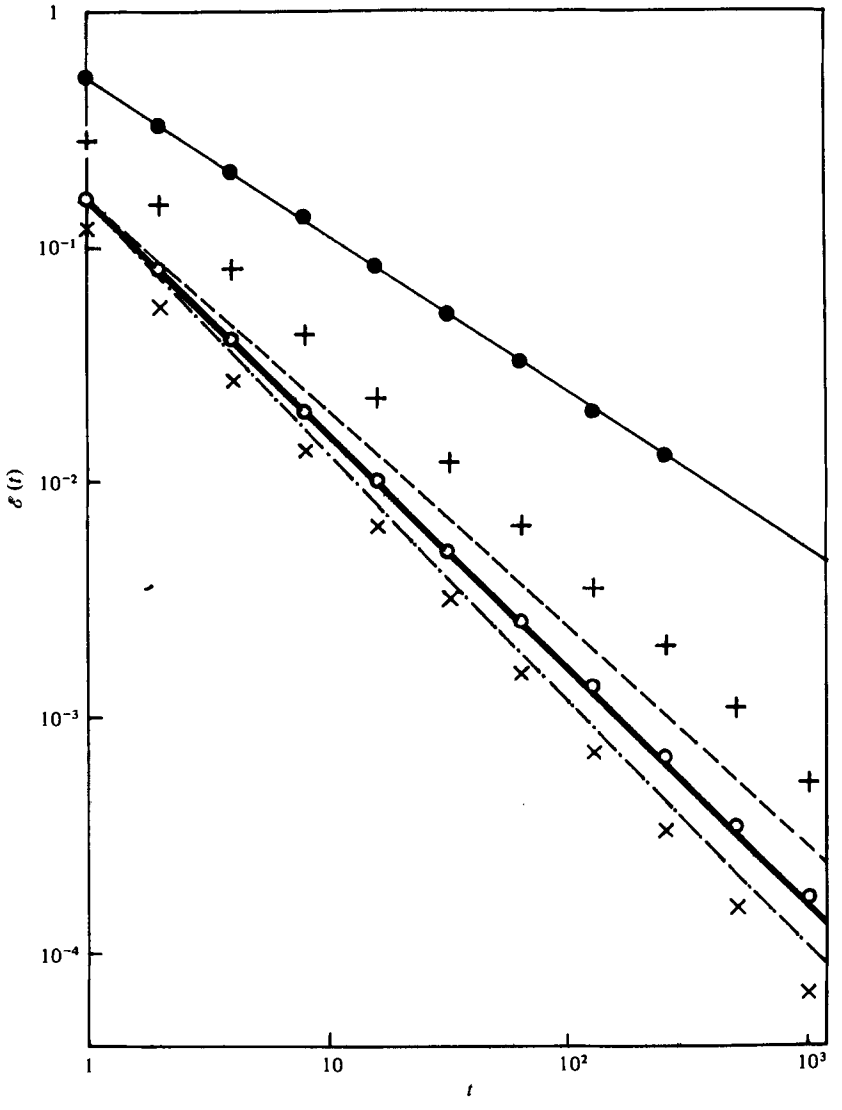

FIGURE 13. The time-dependence of the turbulent energy per unit length.

together with the analytical energy decay curves derived from (4.24), (4.28) and (7.11). The agreement of the numerical and analytical results is again good in experiment (ii). But just as for the characteristic length $l(t)$ it is seen that the energy decay curves for experiments (i) and (iii) are slightly diverse from the corresponding analytical ones though they have the same time-dependence.

The velocity correlation function is calculated through (7.8). The integration with respect to $\tilde{r}'$ is carried out by making use of the trapezoidal rule with the step 0·05. The Fourier transformation (7.19) of the velocity correlation function yields the energy spectrum function. These functions at $t = 1$ are plotted in figures 10 and 11, respectively. Here again we observe the good agreement for experiment (ii) and slight disagreement for (i) and (iii). This disagreement may be attributed to the fact that $\Delta x = 0{\cdot}01$ for (i) and (iii) is not sufficiently small to realize the asymptotic states. The

above results show that the approach to the asymptotic states is very slow except for experiment (ii).

8.2. *Case* II: $J \neq 0$

Next we shall consider the case $J \neq 0$ which was investigated analytically by Burgers (1974). Except for the fact that the series of contact points is expressed as a Wiener-process along the x axis, the analysis is just the same as the present one for the case $J = 0$. Thus we shall recapitulate only his results which are related to the present work.

Let $P(x', y'|x, y)$ be the transition probability of the Wiener-process from the point (x, y) to (x', y'). Then taking account of (3.5), we have

$$P(x', y'|x, y) = \left(\frac{1}{4\pi J|x'-x|}\right)^{\frac{1}{2}} \exp\left[-\frac{(y'-y)^2}{4J|x'-x|}\right]. \tag{8.2}$$

The absolute position of the series of contact points described by this process is indefinite. But it does not matter, for the velocity field is determined completely only by the form of the series. It should be noted that although the probability distribution of the series is inhomogeneous along the x axis, the velocity field derived from it is homogeneous.

The characteristic length $l(t)$ and the turbulent energy per unit length $\mathscr{E}(t)$ are immediately obtained by making use of the constancy of J and the dimensional reasoning as follows:

$$l(t) \propto t^{\frac{2}{3}}, \quad \mathscr{E}(t) \propto t^{-\frac{2}{3}}. \tag{8.3}$$

The highest parabolic arcs are determined in the same way as in § 8.1. Statistics of them yields various probability distribution functions for shocks. Actually, Burgers expressed the joint probability distribution function for μ and ζ of a single shock in an integral form, but the expression was too complicated to be drawn graphically. Therefore only a few lower-order moments $\langle \mu^m \zeta^n \rangle$ were calculated as listed in table 2.† The constants m_1, m_3 and m_5 were expressed by complicated series. The first two of them were estimated approximately as follows, but m_5 has not yet been worked out:

$$m_1 \approx 1{\cdot}053, \quad m_3 \approx 1{\cdot}8. \tag{8.4}$$

It follows from homogeneity and isotropy of the velocity field that

$$\langle \mu^m \zeta^n \rangle = 0 \quad \text{when } n \text{ is odd.} \tag{8.5}$$

The characteristic length $l(t)$ and the turbulent energy per unit length $\mathscr{E}(t)$ are obtained by making use of the values of $\langle \tilde{\mu} \rangle$, $\langle \tilde{\mu}^3 \rangle$ and $\langle \tilde{\mu} \tilde{\zeta}^2 \rangle$ and their time-dependences (8.3) as follows:

$$l(t) = \frac{1}{m_1} t^{\frac{2}{3}}, \tag{8.6}$$

$$\mathscr{E}(t) = \tfrac{1}{2} m_1 J^{\frac{2}{3}} t^{-\frac{2}{3}}. \tag{8.7}$$

The numerical experiments are made for the purpose of confirming the above predictions and determining numerical values of various statistical quantities whose explicit forms are not yet obtained analytically, such as the distribution functions for

† In this subsection the variables $\tilde{\mu}$, $\tilde{\xi}$, $\tilde{\lambda}$, $\tilde{r}$ stand for the corresponding ones measured by $J^{\frac{1}{3}}t^{\frac{2}{3}}$ and $\tilde{f}$, $\tilde{g}_a$, $\tilde{g}_s$, $\tilde{g}$, $\tilde{h}$ the functions of these variables.

	n		
m	0	2	4
0	1	$\frac{m_3}{2m_1}(\doteqdot 0{\cdot}85)$	$\frac{125}{42m_1}+\frac{11m_5}{40m_1}$
1	$\frac{1}{m_1}(\doteqdot 0{\cdot}950)$	$\frac{8}{9}(\doteqdot 0{\cdot}667)$	—
2	$\frac{m_3}{m_1}(\doteqdot 1{\cdot}7)$	$\frac{34}{21m_1}+\frac{m_5}{5m_1}$	—
3	4	—	—
4	$\frac{296}{21m_1}+\frac{m_5}{m_1}$	—	—
5	$\frac{20m_3}{m_1}(\doteqdot 34)$	—	—

TABLE 2. Several lower-order moments $\langle\tilde{\mu}^m\tilde{\zeta}^n\rangle = \langle\mu^m\zeta^n\rangle/(J^{\frac{1}{2}}t^{\frac{3}{2}})^{m+n}$ obtained by Burgers (1974) where $m_1 \approx 1{\cdot}053$ and $m_3 \approx 1{\cdot}8$ but m_5 is not yet known.

shocks, the velocity correlation function and the energy spectrum function. The procedure of the experiments is the same as that in §8.1 except that the probability distribution function (8.2) is adopted here for setting up the series of contact points.

Just like in §8.1 it turns out that all the statistical quantities are self-preserving with respect to time. But a weak dependence of the characteristic length on the step width Δx is observed. It is obvious from the way how the s curve is set up that the shocks whose strengths are less than $\Delta x/t$ are disregarded in the velocity field. The fraction of such shocks is equal to that of the Wiener-process which oozes through the space of the discrete points (4.1). By taking account of spreading of the Wiener-process, we can expect that the fraction is proportional to the square root of Δx. Therefore the number density of shocks may be expressed as a linear function of $(\Delta x)^{\frac{1}{2}}$ when $\Delta x \ll 1$. In order to examine the dependence of the number density on Δx and extrapolate the characteristic length at the limit $\Delta x = 0$ we make eleven experiments with different Δx. Actually $(\Delta x)^{\frac{1}{2}} = 0{\cdot}1 + 0{\cdot}02n$, $n = 0, 1, 2, \ldots, 10$ are chosen. For each fixed Δx ten independent experiments are made and the numerical values of all the statistical quantities are obtained by taking an ensemble average over them.

The number density of shocks at $t = 1$ is plotted against the square root of Δx in figure 14. It is seen that they lie on a common straight line though there exist some statistical fluctuations. The full line is the one which is determined by the method of least squares:

$$N_{\Delta x}(1) = 1{\cdot}058 - 0{\cdot}425(\Delta x)^{\frac{1}{2}}. \tag{8.8}$$

Thus, at the limit $\Delta x = 0$ we have

$$N(1) = m_1 \approx 1{\cdot}058. \tag{8.9}$$

The characteristic length at $t = 1$ is given by the reciprocal of (8.9):

$$l(1) \approx 0{\cdot}945. \tag{8.10}$$

The agreement with (8.4) and (8.6) is quite satisfactory.

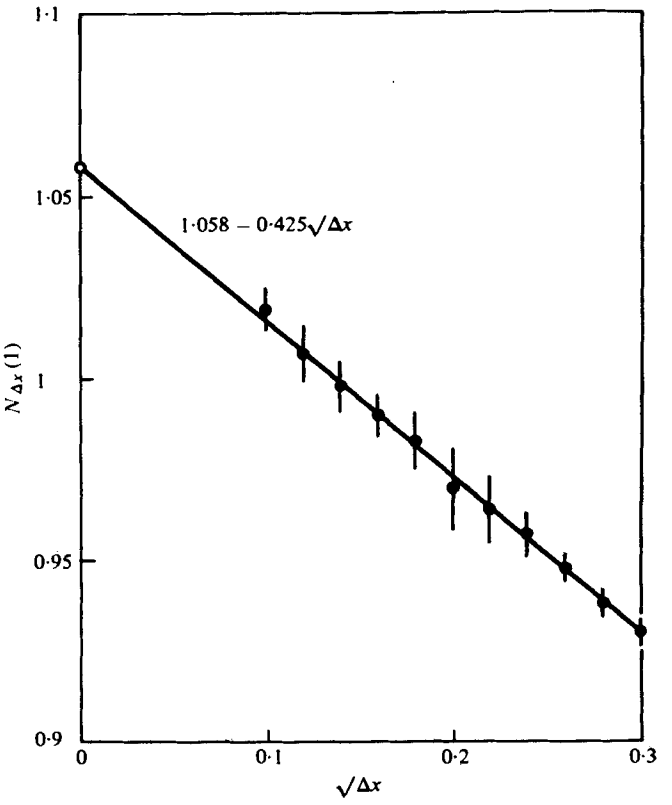

FIGURE 14. The dependence of the number density on the step Δx. The dots and the vertical lines indicate the mean value and the standard deviation. The full line is determined by means of the method of least squares.

In the following we shall show the modified data in the experiment with $\Delta x = 0{\cdot}01$, in which the number density at $t = 1$ happened to be 1·019. All the statistical quantities are modified by multiplying the factor $1{\cdot}019/1{\cdot}053 \approx 0{\cdot}968$ in order to obtain the limiting values at $\Delta x = 0$.

The characteristic length $l(t)$ and the turbulent energy per unit length $\mathscr{E}(t)$ are plotted together with the analytical results (8.6) and (8.7) in figures 12 and 13, respectively. It is seen that the experimental and analytical results are in good agreement.

Several lower-order moments $\langle \tilde{\mu}^m \tilde{\xi}^n \rangle$ for even n at $t = 1$ are listed in table 3. It is seen that in this case the distributions for $\tilde{\mu}$ and $\tilde{\xi}$ are not independent of each other, i.e. $\langle \tilde{\mu}^m \tilde{\xi}^n \rangle \neq \langle \tilde{\mu}^m \rangle \langle \tilde{\xi}^n \rangle$. They are in good agreement with those in table 2 within the statistical fluctuations. By making comparison between these two tables we find

$$m_3 = 1{\cdot}79 \pm 0{\cdot}02 \quad \text{and} \quad m_5 = -2{\cdot}6 \pm 0{\cdot}1, \tag{8.11}$$

where m_3 agrees with the analytical value (8.4). Incidentally it is observed that the moments for odd n fluctuate about zero.

The statistical functions are determined numerically by taking an ensemble average over ten experiments. The standard deviations are on the whole within a few per cent of the mean values. Since all the functions are self-preserving with respect to time, we shall show the data at $t = 1$.

	n		
m	0	2	4
0	1	$0{\cdot}828 \pm 0{\cdot}007$	$2{\cdot}12 \pm 0{\cdot}05$
1	0·950	$0{\cdot}666 \pm 0{\cdot}005$	$1{\cdot}44 \pm 0{\cdot}03$
2	$1{\cdot}70 \pm 0{\cdot}02$	$1{\cdot}06 \pm 0{\cdot}02$	$2{\cdot}04 \pm 0{\cdot}05$
3	$3{\cdot}98 \pm 0{\cdot}08$	$2{\cdot}26 \pm 0{\cdot}05$	$4{\cdot}0 \pm 0{\cdot}2$
4	$10{\cdot}9 \pm 0{\cdot}3$	$5{\cdot}8 \pm 0{\cdot}2$	$9{\cdot}5 \pm 0{\cdot}5$
5	34 ± 1	$17{\cdot}3 \pm 0{\cdot}6$	26 ± 2

TABLE 3. Several lower-order moments $\langle \tilde{\mu}^m \tilde{\zeta}^n \rangle$ determined by taking an ensemble average over ten numerical experiments, where $\pm$ stands for the standard deviation.

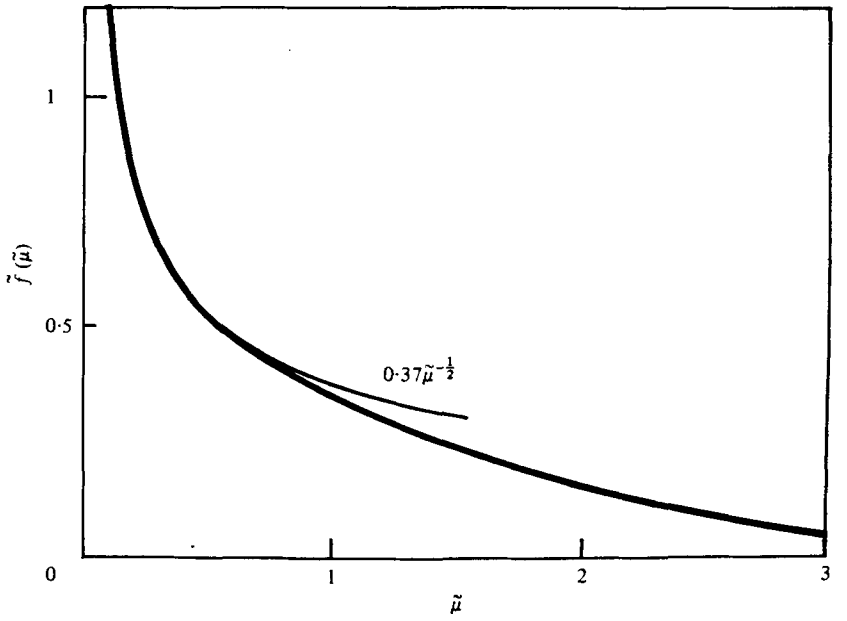

FIGURE 15. The probability distribution for the strength of shocks for case II.

The distribution function for the strength of shocks $\tilde{f}(\tilde{\mu})$ is depicted in figure 15. It diverges to infinity at $\tilde{\mu} = 0$. A closer inspection reveals that

$$\tilde{f}(\tilde{\mu}) \approx 0{\cdot}37\tilde{\mu}^{-\frac{1}{2}} \quad \text{as} \quad \tilde{\mu} \to 0, \tag{8.12}$$

which is compatible with (8.8) since, when a function which behaves like $\tilde{\mu}^{-\frac{1}{2}}$ is approximated by a step function of width Δx, an error proportional to $(\Delta x)^{\frac{1}{2}}$ may occur.

The distribution function for the advance velocity of shocks $\tilde{h}(\tilde{\zeta})$ is plotted in figure 16. A Gaussian distribution with the same variance is drawn by a full line for comparison. The good agreement suggests that $\tilde{h}(\tilde{\zeta})$ can be approximated by a Gaussian distribution, but this is not yet proved analytically.

The distributions for the distance between two adjacent and separated shocks and their sum, $\tilde{g}_a(\tilde{\lambda})$, $\tilde{g}_s(\tilde{\lambda})$ and $\tilde{g}(\tilde{\lambda})$ respectively, are depicted in figure 17. They are somewhat similar to those for the case $J = 0$. It is observed that $\tilde{g}_a(0)$ coincides with the

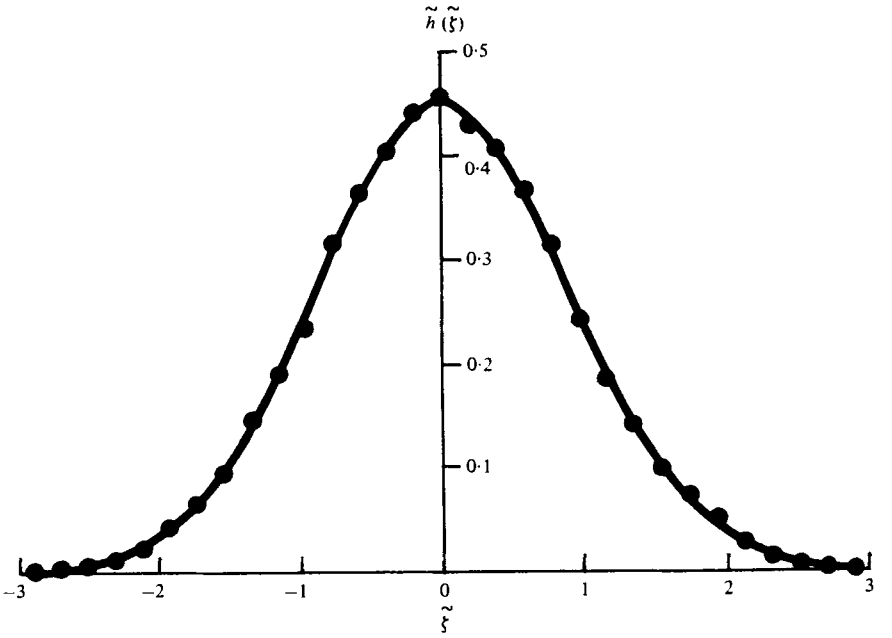

FIGURE 16. The probability distribution for the advance velocity of shocks for case II. The full line denotes a Gaussian distribution with the same variance.

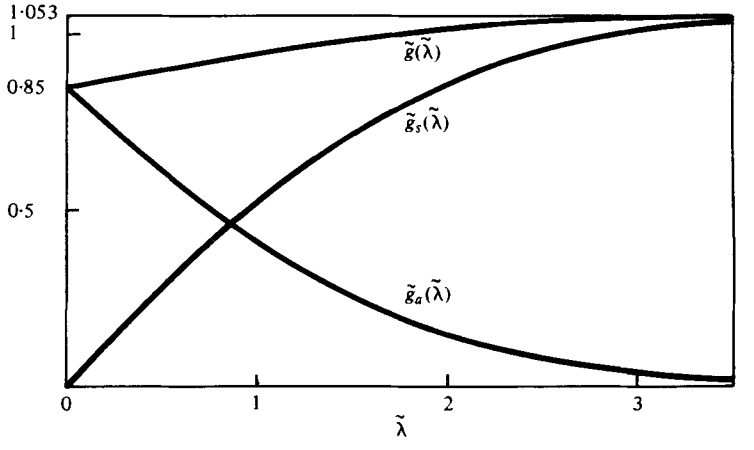

FIGURE 17. The probability distributions for the distance between two shocks for case II.

value $m_3/2m_1 \approx 0{\cdot}85$ which was obtained by Burgers, $\tilde{g}_s(\tilde{\lambda})$ increases in proportion to $\tilde{\lambda}$ near the origin and $\tilde{g}(\tilde{\lambda})$ approaches $N(1) = 1{\cdot}053$ as $\tilde{\lambda} \to \infty$.

The velocity correlation function $B(r,t)$ is shown in figure 18, where

$$\tilde{B}(\tilde{r}) = (t/J)^{\frac{2}{3}} B(r,t). \tag{8.13}$$

This function is positive definite for all $\tilde{r}$ and coincides near $\tilde{r} = 0$ with the line

$$\tilde{B}(\tilde{r}) = 1{\cdot}053 - 0{\cdot}9\tilde{r}, \tag{8.14}$$

which is derived analytically from (7.8) and table 2.

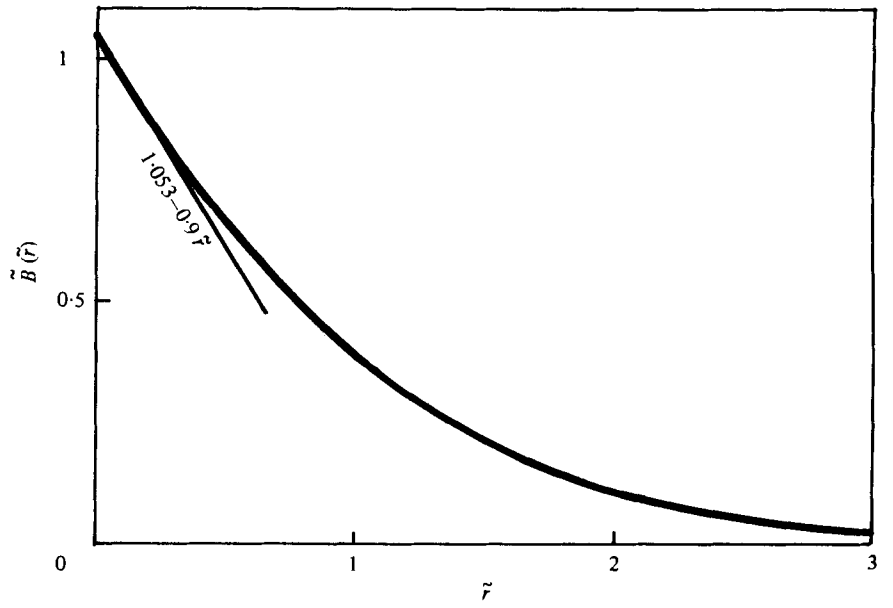

FIGURE 18. The velocity correlation function for case II.

Figure 19 shows the energy spectrum function $E(k,t)$ obtained by the Fourier transformation (7.19) of $B(r,t)$. The normalized wavenumber $\tilde{k}$ and the normalized energy spectrum $\tilde{E}(\tilde{k})$ are defined by

$$\tilde{k} = J^{\frac{1}{2}}t^{\frac{3}{2}}k, \quad \tilde{E}(\tilde{k}) = \frac{1}{J}E(k,t). \tag{8.15), (8.16}$$

At large wavenumbers the energy spectrum function has the asymptote

$$\tilde{E}(\tilde{k}) \approx 0{\cdot}29\tilde{k}^{-2}, \tag{8.17}$$

which is derived analytically from (7.29) and table 2. Here again Kolmogorov's $k^{-\frac{5}{3}}$ energy spectrum is not observed. At small wavenumbers it approaches the constant value $1/\pi \approx 0{\cdot}318$ which follows from (7.27) and the definition of J. Our energy spectrum function bears a close resemblance to those obtained by Jeng *et al.* (1966) and Hosokawa & Yamamoto (1970). Since, however, the time-dependence of the length-scales in these earlier works is unknown, quantitative comparison with them is not possible.

9. Discussion

The asymptotic properties of Burgers turbulence at extremely large Reynolds numbers and times have been investigated by dealing with an ensemble of solutions of the Burgers equation as the initial value problem. It is found that some of them depend crucially upon the statistical properties of the initial velocity field. For example, the characteristic length and the turbulent energy per unit length change in time in different manners in cases I and II (see table 4). In this section we shall give another interpretation to their time-dependences by making use of the geometrical procedure of constructing solutions in terms of the s curve and the parabolic arcs.

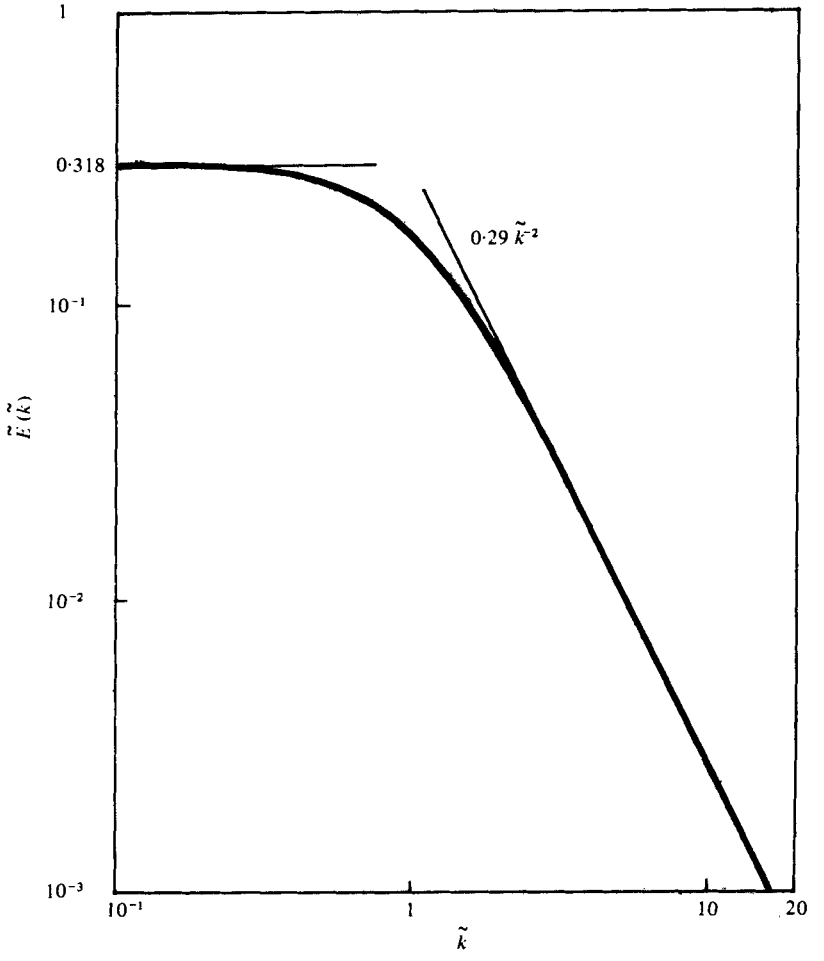

FIGURE 19. The energy spectrum function for case II.

Case	J	σ	$l(t)$	$\mathscr{E}(t)$	$E(k, t)$ for small k
I	0	0	$t^{\frac{1}{2}}$	t^{-1}	k^2
II	Finite	$\frac{1}{2}$	$t^{\frac{2}{3}}$	$t^{-\frac{4}{3}}$	Constant
III	Infinite	1	t	Divergent	k^{-2}

TABLE 4. The characteristics of turbulence dependent upon J.

An s curve which starts from the origin fluctuates at random about the x axis and its mean extent, which is measured by the root mean square distance from the x axis, increases with x. Let us suppose the mean extent of the s curve changes with x as

$$y \propto x^{\sigma}, \tag{9.1}$$

where $\sigma \geqslant 0$ (figure 20). Here we confine ourselves to the case in which the probability of finding the s curve at (x, y) decreases rapidly, e.g. exponentially as y goes to infinity. For, when it decreases slowly, e.g. algebraically, the s curve spreads out gently and its extent is not definite.

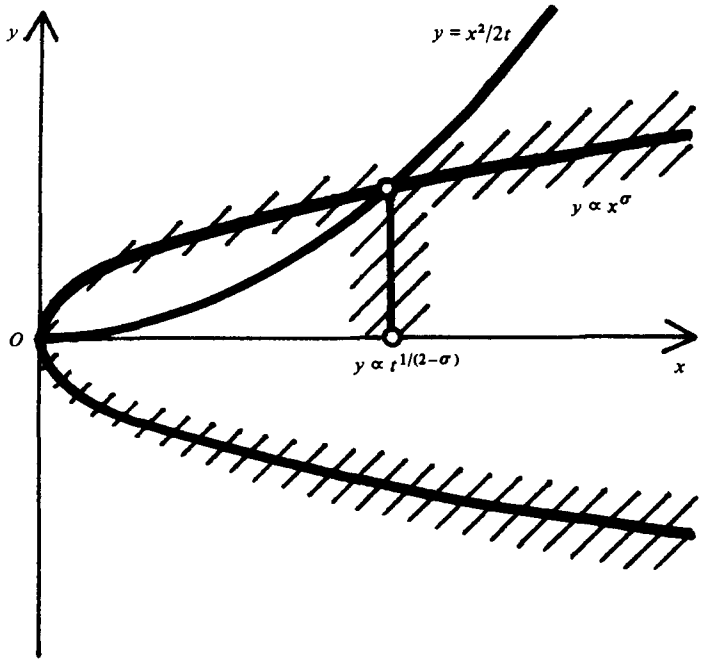

FIGURE 20. The geometrical interpretation of the time-dependence of the characteristic length.

Remember that the characteristic length is given by the mean distance between two adjacent contact points of the s curve on the parabolic arcs. Since the contact points come close to the tops of the parabolic arcs at large times, the order of the characteristic length may be measured by the x co-ordinate of the intersection of the parabola

$$y = x^2/2t \tag{9.2}$$

and the extent of the s curve (9.1), both of which pass through the origin. Then we find

$$l(t) \propto t^{1/(2-\sigma)}. \tag{9.3}$$

Now let us consider the following three cases: (I) the probability distribution for

$$s(x) = -\int^x u(x', 0)\, dx'$$

is homogeneous, (II) $u(x, 0)$ is homogeneous and (III) $\partial u(x, 0)/\partial x$ is homogeneous. The first two are equivalent to cases I and II in the previous sections respectively. The parameters σ corresponding to the cases I, II, III are 0, $\frac{1}{2}$, 1, respectively. The last two values of σ are derived by taking the law of large numbers into account. The time-dependences of $l(t)$ and $\mathscr{E}(t)$ for the respective cases are listed in table 4. It is seen that they coincide perfectly with the previous results in cases I and II. Recently the numerical experiments corresponding to case III were made by Tokunaga (1979) and it was observed that $l(t) \propto t$. Incidentally, in this case the turbulent energy per unit length diverges to infinity, and so does J.

In the present paper the velocity correlation function $\langle u(x,t)\, u(x+r,t)\rangle$ has been calculated by making use of the joint probability distribution for two shocks. The two-point velocity correlation functions of arbitrary order $\langle u(x,t)^m u(x+r,t)^n\rangle$,

$m, n = 1, 2, 3, \ldots$, can be calculated in the same way. But in order to obtain three- or more-point velocity correlation functions it is necessary to know the joint probability distributions for the corresponding numbers of shocks.

Lastly we should like to make a remark on the behaviour of the energy spectrum function $E(k,t)$ for small wavenumbers. It has a close relation to the asymptotic behaviour of the velocity correlation function $B(r,t)$ for large r.

When $B(r,t)$ falls to zero faster than any negative power of r, any order of moments of $B(r,t)$ exists and therefore $E(k,t)$ is infinitely differentiable with respect to k at $k = 0$. Then $E(k,t)$ can be expanded into a power series of k as follows:

$$E(k,t) = E_0 + E_2(t)\,k^2 + E_4(t)\,k^4 + \ldots. \tag{9.4}$$

The lack of odd-power terms is due to the fact that $E(k,t)$ is an even function of k and infinitely differentiable with respect to k at $k = 0$. Although $E_0 = J/\pi$ is a constant of motion, it is not known whether E_{2n} $(n \neq 0)$ are invariant in time or not. It is very probable that they may change in time except for the cases of some particular initial conditions. Therefore it may be assumed that E_{2n} $(n \neq 0)$ take non-zero values even if they are put at zero at an initial instant. Consequently we have, in general,

$$E(k,t) \propto k^2 \quad \text{or} \quad E(k,t) \approx \text{constant}\,(\neq 0)$$

for small k according as $E_0 = 0$ or $E_0 \neq 0$. These correspond to cases I and II, respectively. In passing, we may point out that $E(k,t) \propto k^{-2}$ for small k in case III. In this case the spectrum function of $\partial u(x,t)/\partial x$ takes a finite value at the zero wavenumber.

When $B(r,t) \sim O(r^{-s})$ $(s > 1)$ for large values of r, on the other hand, the situation is quite different. If we denote the least integer not less than s by n, $E(k,t)$ is $(n-2)$ times differentiable with respect to k at $k = 0$. Then we have

$$E(k,t) = E_0 + E_2(t)\,k^2 + \ldots + E_{N-2}(t)\,k^{N-2} + Res, \tag{9.5}$$

where N is the largest even number not larger than n and

$$Res = \begin{cases} O(k^{n-1}\ln k) & \text{when } s \text{ is an integer,} \\ O(k^{s-1}) & \text{otherwise.} \end{cases} \tag{9.6}$$

It is possible that in this case $E(k,t)$ begins with powers other than even numbers. In fact, when $E_0 = 0$, we have $E(k,t) \propto k^{s-1}$ or $E(k,t) \propto k^2$ for small k according as

$$1 < s < 3 \quad \text{or} \quad s > 3.$$

In order to investigate the dependence of the energy decay law on the large-scale motion of turbulence, i.e. the form of $E(k,t)$ for small k, Yamamoto & Hosokawa (1976) made numerical experiments using the initial energy spectrum of the type $k^a \exp(-k^2)$, $a = 0, \frac{1}{8}, \frac{1}{2}, 2, 10, 18$. To our great regret, however, the results are not decisive. The states in which any power law holds were not attained in their experiments probably because Reynolds numbers and/or times were not sufficiently large. The numerical experiments with larger Reynolds numbers and times are eagerly waited for. It is very interesting to know what kind of difference would be realized according as $B(r,t)$ falls to zero faster than any negative power of r with increasing r or not.

Appendix

We give here another derivation of the energy decay law in case I, which is chiefly due to U. Frisch (1978).

Let us introduce a velocity potential $a(x,t)$ such that

$$u(x,t) = -\frac{\partial}{\partial x}a(x,t). \tag{A 1}$$

Assume that initially

$$u(x,0) = -\frac{\partial}{\partial x}a_0(x), \tag{A 2}$$

where $a_0(x)$ is a spatially stationary stochastic process. Then $a(x,t)$ obeys

$$\frac{\partial}{\partial t}a = \frac{1}{2}\left(\frac{\partial a}{\partial x}\right)^2 + \frac{1}{R}\frac{\partial^2 a}{\partial x^2}, \tag{A 3}$$

which is derived from (A 1) and the Burgers equation (2.1). Notice that $a_0(x)$ is equivalent to the s curve $s(x)$. Since (A 3) is translation-invariant, $a(x,t)$ will be a spatially stationary process for any t (> 0). Averaging (A 3), we find that

$$\mathscr{E}(t) = \tfrac{1}{2}\langle u(x,t)^2\rangle = \frac{1}{2}\left\langle\left(\frac{\partial a}{\partial x}\right)^2\right\rangle = \frac{\partial}{\partial t}\langle a(x,t)\rangle. \tag{A 4}$$

Therefore the energy decay law can be obtained from the time derivative of the mean potential. In the limit $R\to\infty$, the velocity potential has a simple representation

$$a(x,t) = \sup_{x'}\left\{a_0(x') - \frac{(x-x')^2}{2t}\right\}. \tag{A 5}$$

This follows from the same argument as that described below (2.2).

In order to calculate $\langle a(x,t)\rangle$ ($= \langle a(0,t)\rangle$), we define the distribution function for a:

$$Q(a,t) = \text{Prob}\{a(0,t) < a\} = \text{Prob}\left\{a_0(x') - \frac{x'^2}{2t} < a \text{ for all } x'\right\}. \tag{A 6}$$

Then we have

$$\langle a(x,t)\rangle = \int_{-\infty}^{\infty} a\frac{\partial Q}{\partial a}da = \int_{-\infty}^{\infty}\{H(a) - Q(a,t)\}\,da, \tag{A 7}$$

where $H(a)$ is the Heaviside function, and $Q(-\infty,t) = 0$ and $Q(\infty,t) = 1$ have been taken into account. The time derivative of (A 7) yields the turbulent energy

$$\mathscr{E}(t) = -\int_{-\infty}^{\infty}\frac{\partial}{\partial t}Q(a,t)\,da. \tag{A 8}$$

It can be shown that, when $t \gg 1$, the function $Q(a,t)$ only for very large a (say $a \gg \langle a^2\rangle^{\frac{1}{2}}$) will be requisite. Then, in just the same way as in § 4, we find

$$Q(a,t) = \exp\left[-\frac{\sqrt{(2t)}}{\Delta x}\int_{-\infty}^{\infty}F(x^2+a)\,dx\right]. \tag{A 9}$$

Substitution of (A 9) into (A 8) leads to

$$\mathscr{E}(t) = \frac{1}{\Delta x(2t)^{\frac{1}{2}}}\int_{-\infty}^{\infty}\left\{\int_{-\infty}^{\infty}F(x^2+a)\,dx\exp\left[-\frac{(2t)^{\frac{1}{2}}}{\Delta x}\int_{-\infty}^{\infty}F(x^2+a)\,dx\right]\right\}da. \tag{A 10}$$

When $P(y)$ is given by (4.15), we obtain

$$\mathscr{E}(t) \propto t^{-1} (\ln t)^{(1-\beta)/\beta} \approx t^{-1}, \tag{A 11}$$

which is the same as (7.12). For the algebraic decrease case

$$P(y) \propto y^{-\gamma} \quad \text{as} \quad y \to \infty, \tag{A 12}$$

on the other hand, we get

$$\mathscr{E}(t) \propto t^{-2(\gamma-2)/(2\gamma-3)}. \tag{A 13}$$

The power in (A 13) varies between $-\frac{1}{2}$ and -1, since $\gamma > \frac{5}{2}$ is required to ensure the convergence of the integral in (A 10).

The same energy decay law can be, of course, obtained by direct integration, not by the method of steepest descent, in the framework in the previous sections. Furthermore, it can be shown that in the case of (A 12) the velocity correlation function $B(r, t)$ vanishes algebraically like $r^{5-2\gamma}$ as $r \to \infty$. This behaviour is quite different from that in the case of exponential decrease of $P(y)$. The details in the case of (A 12) will be studied elsewhere.

The author would like to express his cordial thanks to Prof. T. Tatsumi for his continual guidance and helpful advice and Prof. U. Frisch for his invaluable comments.

REFERENCES

BURGERS, J. M. 1950 Correlation problem in a one-dimensional model of turbulence. *Proc. Amsterdam* **53**, 393–406.

BURGERS, J. M. 1974 *The Nonlinear Diffusion Equation*. D. Reidel Publishing Co.

COLE, J. D. 1951 On a quasi-linear parabolic equation occurring in aerodynamics. *Quart. Appl. Math.* **9**, 225–236.

CROW, S. C. & CANAVAN, G. H. 1970 Relation between a Wiener–Hermite expansion and an energy cascade. *J. Fluid Mech.* **41**, 387–403.

FRISCH, U. 1978 Private communication.

HOPF, E. 1950 The partial differential equation $u_t + uu_x = u_{xx}$. *Commun. Pure Appl. Mech.* **3**, 201–230.

HOSOKAWA, I. & YAMAMOTO, K. 1970 Numerical study of Burgers' model of turbulence based on the characteristic functional formalism. *Phys. Fluids* **13**, 1683–1692.

JENG, D. T., FOERSTER, R., HAALAND, S. & MEECHAM, W. C. 1966 Statistical initial-value problem for Burgers' model equation of turbulence. *Phys. Fluids* **9**, 2114–2120.

KAWAHARA, T. 1968 A successive approximation for turbulence in the Burgers model fluid. *J. Phys. Soc. Japan* **25**, 892–900.

KOLMOGOROV, A. N. 1941 The local structure of turbulence in incompressible viscous fluid for very large Reynolds numbers. *C. R. Acad. Sci. U.R.S.S.* **30**, 301–305.

KOLMOGOROV, A. N. 1962 A refinement of previous hypotheses concerning the local structure of turbulence in a viscous incompressible fluid at high Reynolds number. *J. Fluid Mech.* **13**, 82–85.

KRAICHNAN, R. H. 1968 Lagrangian-history statistical theory for Burgers' equation. *Phys. Fluids* **11**, 265–277.

LIGHTHILL, M. J. 1956 Viscosity effects in sound waves of finite amplitude. In *Surveys in Mechanics* (ed. G. K. Batchelor and R. M. Davies), pp. 250–351. Cambridge University Press.

MALFLIET, W. P. M. 1969 A theory of homogeneous turbulence deduced from the Burgers equation. *Physica* **45**, 257–271.

MEECHAM, W. C. & SIEGEL, A. 1964 Wiener–Hermite expansion in model turbulence at large Reynolds numbers. *Phys. Fluids* **7**, 1178–1190.

REID, W. H. 1957 On the transfer of energy in Burgers' model of turbulence. *Appl. Sci. Res.* A **6** 85–91.

TATSUMI, T. 1969 Nonlinear wave expansion for turbulence in the Burgers' model of fluid. *Phys. Fluids Suppl.* II **12**, 258–264.

TATSUMI, T. & KIDA, S. 1972 Statistical mechanics of the Burgers model of turbulence. *J. Fluid Mech.* **55**, 659–675.

TATSUMI, T. & MIZUSHIMA, J. 1979 Submitted to *J. Fluid Mech.*

TATSUMI, T. & TOKUNAGA, H. 1974 One-dimensional shock turbulence in a compressible fluid. *J. Fluid Mech.* **65**, 581–601.

TOKUNAGA, H. 1979 To be published.

YAMAMOTO, K. & HOSOKAWA, I. 1976 Energy decay of Burgers' model of turbulence. *Phys. Fluids* **19**, 1423–1424.